POLITECNICO
MILANO 1863

SCUOLA DI INGEGNERIA INDUSTRIALE
E DELL'INFORMAZIONE

# Validation and use of Teslasuit in a virtual-reality environment for neuromotor rehabilitation: a proof of concept study on healthy subjects

Tesi di Laurea Magistrale in
Biomedical Engineering - Ingegneria Biomedica

**Giulia Lomele, 970995**
**Francesca Lucchetti, 968545,**

**Advisor:**
Prof. Emilia Ambrosini

**Co-advisors:**
Francesca Dell'Eva

**Academic year:**
2022-2023

**Abstract:** Stroke is a leading cause of mortality and disability in the European Union, frequently resulting in hemiparesis of the limbs contralateral to the brain lesion. Post-stroke rehabilitation is essential for restoring neuromuscular function and achieving independence in daily activities.
In recent years, innovative integrated devices have emerged as promising tools in this field, such as the full-body suit, named Teslasuit, which combines Neuromuscular Electrical Stimulation, IMU-based Motion Capture, and Virtual Reality.
The present study investigates Teslasuit's potential in post-stroke upper limb rehabilitation, aiming to validate its efficacy and assess its feasibility for medical applications. This study proposes validation protocols for both Teslasuit's motion capture and electrical stimulation systems and an imitation-based exercise protocol, inspired by Mirror Therapy, to be performed in virtual reality environments.
Our results, collected from 5 healthy subjects for each protocol, prove the validity of the suit motion capture system in accurately tracking movements, as well as the effectiveness of the electrical stimulation system, presented as a potential tool for neuromotor rehabilitation. Moreover, the data also demonstrate the feasibility of integrating these systems with VR. In conclusion, this research highlights that Teslasuit holds promise as a versatile and innovative device for implementing upper limb neuromotor rehabilitation therapies.

**Key-words:** FES; Teslasuit; motion capture; virtual reality; integrated wearable devices

## 1. Introduction

A stroke can occur due to an obstruction of blood flow to the brain (ischemic stroke) or an abrupt bleeding within the brain (hemorrhagic stroke). The former results in the deprivation of oxygen and nutrients to the brain cells that thus start dying within minutes; the latter, instead, in a high pressure exerted by the blood within the brain on its cells, inflicting significant damages [1].
In the European Union (EU) stroke is a predominant factor leading to mortality and acquired disability among adults [2]. Studies have estimated a 27% increase in stroke cases between 2017 and 2047 as a result of demographic aging and enhanced survival rates [2], leading to a growing need for post-stroke therapy and assistance.
The most common impairment after stroke, occurring at an 80% rate, is hemiparesis of the contralateral upper limb (with respect to the brain damage), causing changes in the muscle strength and tone, loss of dexterity and

coordinated movements, and joint laxity [3]. Stroke rehabilitation focuses on these aspects, aiming to recover the affected neuromuscular functions and achieve independent body control.
However, almost 60% of patients undergoing and completing standard rehabilitation fail to regain some arm dexterity [4]. Compromised motor control of the upper limb strongly affects patients' ability to perform Activities of Daily Living (ADL) independently, increasing the demand for caretakers and healthcare personnel, and thus impairing patients' quality of life.
This emphasizes the need to use effective rehabilitation techniques and motion capture systems for monitoring patient advancements, especially within the acute phase (from 16 hours to 6 months post-stroke), that is the time period in which the augmented exercise therapy is reported to have the most favorable effects on ADLs [5].
The basic principle of most rehabilitation approaches nowadays is motor learning, achieved with repetitive, intense, functional and task-specific training [6], which facilitates motor recovery by inducing neuroplasticity processes in the brain (i.e., cortical reorganization). Many motor learning-based rehabilitation strategies have been developed in the last several decades, ranging from straightforward ones, such as Constraint-Induced Movement Therapy (CIMT) and Mirror Therapy, to more advanced ones, like Robotic Training and Functional Electrical Stimulation (FES).
Constraint-Induced Movement Therapy (CIMT) aims at preventing the appearance of the "learned non-use", which is the patient tendency to use their non-paretic limb to perform daily activities. To do this, it simply restrains the non-paretic arm while the patient engages in repetitive-intensive functional tasks [6][7].
Mirror Therapy, instead, works on visual stimuli rather than somatosensory ones to produce the desired response in the paretic limb: a mirror placed between the limbs gives the patient the illusion of moving the paretic limb when he is only moving the non-paretic one. This technique was proved to help motor recovery, by engaging the vision sensory system.
Both approaches have been demonstrated to be simple and effective[8][9][10], but, while CIMT presents challenges in wearing the constraint for the prescribed amount of time, involving feelings of fatigue and frustration[11][12], Mirror Therapy does not present any specific contraindication or adverse effect [13].
Moving to the more complex and structured approaches, Robotic Training and FES are gaining increasing attention as alternative methods to more conventional rehabilitation techniques. Robotic training involves robotic devices that allow the patient to perform simple exercises and movement patterns in a controlled and standardized environment. Some very important aspects of this approach are good repeatability, controllable intensity, assistance, or resistance during movements, and the possibility of having objective and quantifiable measures of the subject performance. However, the complexity and encumbrance of the setup prevent this approach from being accepted and applicable to every patient [14].
Lastly, Functional Electrical Stimulation is a technique based on the application of low-energy electrical stimuli to muscles to induce a functional movement. It can be used for enhancing muscle strength, expanding joints' range of motion, countering atrophy, and mitigating pain [15], and it has been reported to clearly improve aspects of ADL performance after stroke [16].
The peculiarity of these approaches is the possibility of combining them with other technologies, including Virtual Reality (VR). This can provide a controlled and safe rehabilitation and learning environment, allowing the modulation of stimuli to tailor the treatment to the individual requirements while motivating the patient by incorporating gaming elements into the rehabilitation process [17].
Another crucial aspect of stroke rehabilitation is the capability of monitoring patients' movement. In this pursuit, emerging technologies like Motion Capture (Mocap) systems play a fundamental role by offering quantitative and systematic standards of evaluation. This technology can capture three-dimensional human motion using optical cameras or Inertial Measurement Unit (IMU) sensors.
The first approach is marker-based and requires a laboratory environment. These settings come with various drawbacks, such as spatial constraints, the necessity for proper lighting and sophisticated calibration, as well as the susceptibility to illumination artifacts due to potential reflective objects or obstructions [18]. Despite these limitations, Optical Motion Capture shows high accuracy in tracking human motion kinematics, hence it is widely regarded as the Gold Standard and thus compared to other Motion Capture Systems. The second approach uses IMU sensors, that combine an accelerometer, a magnetometer and a gyroscope. The main benefits of employing such Mocap Systems include their portability, adaptability, and comfortable wearability. These factors make them suitable for monitoring human motion throughout rehabilitation sessions, even in everyday settings, and easy to incorporate into other electronic systems, like robotic or FES devices [19].
In this direction, new integrated devices are increasingly gaining prominence in the medical and rehabilitation field. These consist of full-body suits that integrate FES systems and/or MoCap systems, resulting in a comprehensive rehabilitative solution, easily applicable in domestic contexts. Teslasuit by VR Electronics and Exopulse Mollii Suit by Ottobock are two examples of full-body suits already on the market. Both incorporate multiple FES electrodes for the stimulation of upper and lower body muscle groups.
The Exopulse Mollii Suit was specifically designed to restore the physiological balance of muscle groups in cases of cerebral palsy, multiple sclerosis, stroke, and other neurological disorders characterized by impaired motor

functions [20]. The Teslasuit, instead, was initially designed to give a four-dimension gaming experience thanks to the presence of a haptic feedback system, an IMU-based Mocap system, and a plugin in Unity, allowing the connection of the suit with a Virtual Reality platform. Now, it is entering the medical and rehabilitation field as a self-standing FES device.

This thesis aims at exploring the usability and performance of Teslasuit as a Functional Electrical Stimulation device, and its feasibility as a medical device in a post-stroke rehabilitation protocol based on the integrated use of FES, Mirror Therapy and Virtual Reality. The thesis is structured in five sections: *Background, Objectives, Materials and Methods, Results and Discussion, Conclusions*. The first provides an overview of the current knowledge about the research topic, the second explores the objectives of the study, the third focuses on the tools used to reach results, which are then described and discussed in the fourth section. To conclude, the last section summarizes the study findings and discusses its implications.

# 2. Background

## 2.1. Functional Electrical Stimulation and Mirror Therapy

### 2.1.1 Functional Electrical Stimulation

Functional Electrical Stimulation consists of applying electrical current pulses to excitable tissue in order to induce an artificial contraction and enhance or replace motor functions in individuals with neurological impairments.

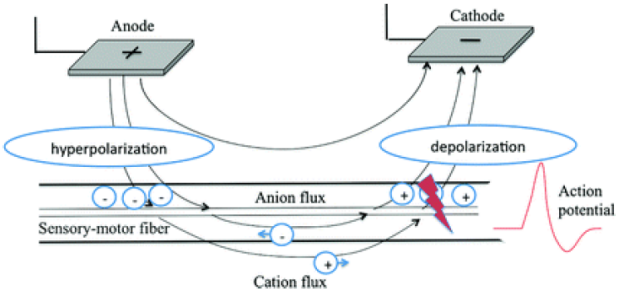


Figure 1: Neurophysiological principles of FES

**Working principle** Stimulation is achieved by applying current through a couple of electrodes placed on the skin overlying sensory-motor structures. The electric field that is established between the two electrodes (anode and cathode) creates an ion flux in the tissue (Figure 1). Specifically, the anode, serving as the positive electrode, imparts a positive charge to the cell membranes of neighboring neurons, leading to an accumulation of negative ions and the consequent membrane hyperpolarization. Conversely, the cathode, that is the negative electrode, attracts positive ions, leading to depolarization of the underlying membrane region. If the depolarization reaches a critical threshold, an action potential is generated, non-distinguishable from the physiological one. The generated action potential propagates to the neuromuscular junction that causes muscle fibers to contract. It is important to specify that the charge threshold necessary for generating action potentials in muscle fibers is notably higher than the one required for neurons. Consequently, electrical stimulation predominantly activates nerves rather than muscles, highlighting the relevance of integer lower motor neurons for FES to be effective [21].

**Muscle recruitment** During an FES-induced contraction, muscle fiber are recruited differently with respect to a physiological one.
First of all, motor units are recruited according to the geometrical activation, from superficial layers at low current levels to deeper ones when increasing the current amplitude [22].
Moreover, while during voluntary movements there is a sequential activation of motor units (asynchronous recruitment), FES recruits all motor units at the same time (synchronous recruitment) [23]. In the asynchronous recruitment, shown in Figure 2 motor units share the work of maintaining a constant tension during the muscle contraction (i.e. tetanic contraction) as adjacent units are activated at a frequency of 6-8 Hz. This also ensures a slower muscle fatigue appearance. Conversely, in the synchronous recruitment, tetanic contractions require a much higher stimulation, up to 20-40 Hz, which is the main cause of the increased rate of muscle fatigue that characterizes FES approaches [22].

Lastly, FES follows a non-physiological recruitment as it recruits fast-twitch fibers before slow-twitch ones because the former are stimulated at lower current thresholds than the latter. This happens because the larger-diameter axons innervating fast-twitch fibers are more affected by the stimulation-induced electric field than the smaller-diameter ones of slow-twitch fibers: the wider space between Ranvier nodes in the former ones produces larger induced transmembrane voltage changes at the same level of charge [21]. However, fast-twitch fibers tend to fatigue quicker and thus the FES non-physiological recruitment contributes to the increased rate of fatigue typical of FES-induced muscle contractions [22].

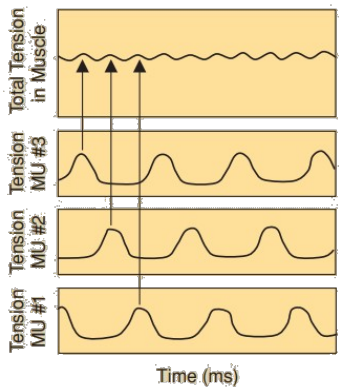


Figure 2: Summation of tension in motor units (MU) during asynchronous recruitment.

**Pulse Shapes** The production of the ionic flux is caused by the variation in the electric field. A relatively rapid rising edge is needed for the current to induce excitation and therefore the stimulus must consist of a properly shaped wave, or pulse [24]. Some of the most common pulse waves used in FES are shown in Figure 3. Waveforms can be divided into monophasic and biphasic. Monophasic ones are characterized by repeated unidirectional pulses, usually cathodic; biphasic ones comprise repeated pulses consisting of a cathodic pulse followed by an anodic one [25]. In the latter configuration, the positive pulse counterbalances the negative one, resulting in a net injected charge equal to zero that prevents potential damages at the electrode-tissue interface [25]. Focusing on biphasic configurations, different types of pulse shapes exist: symmetric, asymmetric and balanced asymmetric. Symmetric pulses consist of two identical phases in terms of duration and amplitude but with opposite polarities. On the contrary, asymmetric pulses comprise phases with different durations and/or amplitudes [26]. Balanced asymmetric shapes, instead, are characterized by proper parameters selection such that the total energy delivered to the body during the leading phase equals the total energy removed from the body during the trailing pulse, despite differing amplitude and duration [26].

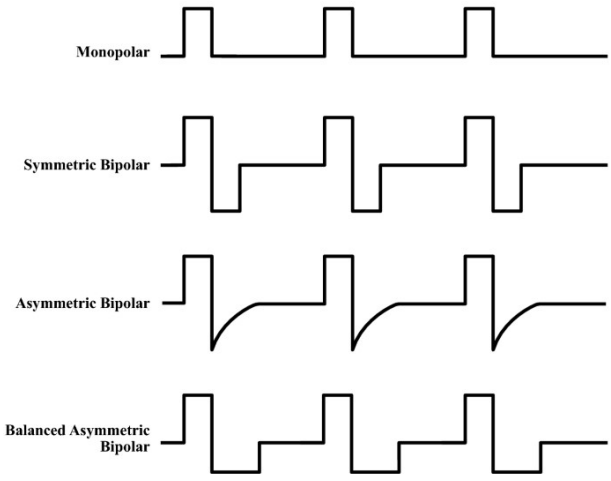


Figure 3: Examples of commonly used pulse shapes used for functional electrical stimulation.

**Stimulation Parameters** FES pulses are characterized by three parameters (as shown in Figure 4): pulse amplitude, pulse duration (or pulse width (PW) ) and pulse frequency [26]. Pulse amplitude is the magnitude of the stimulation and directly impacts the specific type of nerve fibers that respond to it. As above mentioned, larger nerve fibers in close proximity to the stimulation electrode are recruited first [26]. The pulse duration,

or pulse width, is the time duration of a single phase of the pulse. The strength of a pulse is determined by its charge level, which is defined as the product between the pulse amplitude and duration. Thus, the duration required for a pulse to be effective varies in the opposite direction with respect to the amplitude; i.e., to generate the same induced response, an increase in pulse duration requires a lower amplitude and vice versa[26]. Each pulse with proper charge level, allowing to induce an action potential, produces a muscle twitch, characterized by a sharp rise in force followed by a slower return to the relaxed state. The stimulation frequency is the rate at which stimulation pulses are delivered. By increasing it, the temporal summation of twitches results in a higher mean generated force with respect to the one of single twitches [26]. Once the pulse frequency overcomes a certain value (typically 20 Hz), a sustained contraction (defined as tetanic) is obtained, where individual twitches are not distinguishable anymore. This tetanic contraction is achieved with frequency values ranging from 20 to 50 Hz and it is desired in FES applications to provide a high-quality movement. However, pulse frequency should not be excessively increased as it accelerates the appearance of muscle fatigue. Thus, a trade-off is involved in the choice of this parameter [26]. Typical working values are: frequency between 20 and 50 Hz, pulse width between 100 and 500 $\mu$s and amplitude between 10 and 125 mA [25].

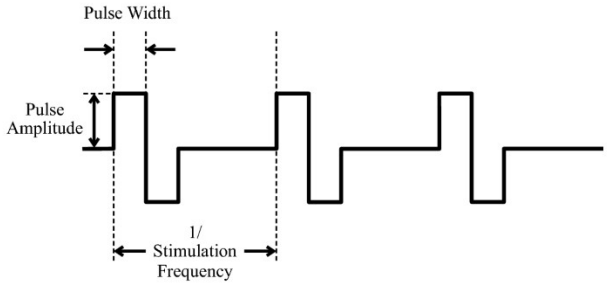


Figure 4: Functional electrical stimulation parameters.

**Stimulator Circuit** Electrical stimulators can deliver either voltage- or current-controlled pulses. Voltage-controlled stimulators provide a constant desired voltage in between electrodes. They do not consider resistance variations in the tissue and thus inadequate skin-electrode contacts, causing an increase in resistance, produce a current decrease and consequently a reduced muscle response, but no potential harm to the skin [27]. Conversely, current-controlled stimulators provide constant current pulses, and in case of reduced effective electrode surface area, current density increases with an increase in the voltage level, leading to potential skin burns [27].

**Benefits** FES-based treatment offers numerous advantages in the rehabilitation process. FES facilitates active muscle contractions, contributes to the enhancement of muscle strength, prevents disuse and muscle atrophy, reduces spasticity and spasms, promotes a more energy-efficient utilization of proximal limb muscles, and diminishes the energy expenditure associated with post-stroke activities [28]. Furthermore, a shift from type IIB to type IIA and type I muscle fibers has been demonstrated [66], indicating improved resistance to fatigue and oxidative capabilities. Despite FES being applied peripherally, several studies have shown that it can induce neurological changes and potentially facilitate motor relearning when combined with residual voluntary inputs from the patient. This phenomenon is commonly referred to in the literature as the "carry-over effect," and its underlying mechanism remains somewhat unclear, though Rushton's hypothesis is widely accepted as the leading explanation. This hypothesis is rooted in the distinctive feature of FES, which activates nerve fibers both orthodromically and antidromically, unlike physiological activation that exclusively operates orthodromically [25], [29].

**Limitations** The main limitations of FES are the non-linear relationship between the injected current and the induced muscle contraction and the early appearance of fatigue induced in stimulated muscles. As previously mentioned, this is due to the different motor units' recruitment, which is synchronous and inverted with respect to the physiological one. This limits the use of FES for long-term applications [30].

### 2.1.2 Mirror Therapy

This method was introduced by Ramachandran and colleagues for individuals with arm amputations. They used the mirror image of the intact arm to simulate the presence of the amputated contralateral limb, getting phantom pain relief in the "virtual" limb. Nowadays Mirror Therapy (MT) has been proposed as an alternative approach to alleviate chronic hemiparesis after stroke since it does not require the patient to have any residual voluntary movement in the affected limb [31].

**Working principle** During the therapy, a mirror is placed in the person's midsagittal plane to create a

reflection of the non-paretic upper or lower limb, giving the person the visual feedback of normal movements coming from the paretic side [31][32].
There is still no unanimous consensus among studies regarding the underlying mechanisms and neurophysiological basis of MT. So far, three hypotheses have been sustained. The first one is the existence of a mirror neuron system (MNS) in the frontotemporal region and the superior temporal gyrus (STG), which activates during goal-oriented actions or while observing similar actions performed by others. This action-observation mechanism enhances the corticospinal pathway, leading to improved motor function by triggering mental imagery and facilitating motor learning [33].
The second hypothesis suggests as potential working mechanisms an enhanced self-awareness and spatial attention through the activation of primary and secondary visual and somatosensory areas (STG, precuneus, and posterior cingulate cortex (PCC)), preventing the development of the learned non-use phenomenon in the affected limb [33].
The third hypothesis suggests an activation of the ipsilateral motor pathways originating from the unaffected hemisphere and projecting ipsilaterally to the weakened side of the body. It has also been postulated that MT plays a role in normalizing the balance between hemispheres by modulating the excitability of the primary motor cortex (M1). In fact, during MT, both the movement of the affected limb and the passive observation of the unaffected limb's movement, as reflected in the mirror, influence M1 excitability [33].

**Benefits** Although the underlying mechanisms of Mirror Therapy have not yet been fully clarified, different studies [34][33][13][35] have stated its effectiveness as a rehabilitation tool. The most significant improvements are generally observed in the patient's movement duration, elbow-shoulder coordination and trajectory accuracy, resulting in an overall enhancement of motor functions. However, contrasting opinions can be found in the literature regarding the enhancement of patients performance in ADLs [33], in fact, some studies report statistically significant differences between pre- and post-therapy outcomes [35], while others do not observe improvements [34].

**Limitations** The above-mentioned improvements seem to be higher in distal arm muscles rather than in proximal ones. One potential explanation for this phenomenon may be the different contributions of the two hemispheres to proximal and distal motor functions: distal ones are organized strictly unilaterally, whereas proximal ones rely more on bihemispheric representations [36].

## 2.2. Virtual Reality

Virtual Reality commonly refers to the use of interactive simulations generated using computer hardware and software. These simulations allow users to engage in controlled environments that closely resemble real-world objects and events. Users can interact with displayed images, manipulate virtual objects, and carry out various actions, all designed to create a sense of immersion within the simulated environment. To enhance the immersive experience, different feedback modalities are employed, including visual, auditory, haptic and vestibular feedback [37]. Nevertheless, immersion represents a complex concept as it depends on different factors.
First of all, the characteristics of the VR system come into play, including the sensor's encumbrance, the visual representation of the user, the supported dimensions of the environment (2-D or 3-D), and the number and quality of feedback modalities. A second set of factors refers to the user's attributes such as age, gender, prior VR experience and disabilities. Lastly, the meaningfulness of the task being undertaken and the realism and intuitiveness of the interactions also contribute to the achievement of the sense of immersion [37].

### 2.2.1 Instrumentation

VR instrumentation is composed of hardware and software components that aim to transfer information from the user to the system and vice-versa. The primary feedback that VR systems usually provide to the user is the visual one, delivered through Head-Mounted Displays (HMDs), projection systems or flat screens [37]. HMDs consist of screens mounted at the eye level within goggles or helmets. They are considered the most immersive option, as they give a view of the virtual environment in very close proximity, sometimes even in three dimensions [37]. Less immersive systems are projection screens and basic desktop monitors, where the virtual environment is respectively projected or displayed. Despite their reduced immersion, these systems are widely adopted in clinics and households due to their cost-effectiveness [37]. Additional forms of feedback can be auditory, delivered through audio displays, or haptic, delivered through haptic displays and force-feedback devices such as joysticks or steering wheels [38]. Regarding the user-environment interaction, two methods exist: the direct and the indirect one. Direct methods consist of systems that track the user's movement and respond accordingly, thanks to the use of specific sensors, like IMU or visual tracking. Sensors generally transmit the position and orientation data to the VR system while in visual tracking, cameras capture a video

that is then processed by a dedicated software to extract the user's real-time image [37]. On the other hand, indirect methods engage computer keyboard keys, a mouse, a joystick or virtual buttons integrated within the simulated environment [39]. Regarding the software, specialized development tools are essential for designing and coding interactive simulated environments that can achieve targeted rehabilitation goals. In those cases where it is necessary to construct a virtual environment from scratch, it may be required to employ conventional programming languages [37].

### 2.2.2 Third and First-person perspectives

Another key aspect is the perspective from which users view the virtual environment as it greatly impacts how they perceive their own body within that environment. Two visual perspectives are generally available, the first-person perspective (1PP) and the third-person perspective (3PP), shown in Figure 5.
The former is achieved by positioning the camera at the avatar's eye level, sometimes also without a representation of the avatar's body. The latter, instead, offers a complete view of the avatar's body movements, with the camera following the avatar at an adjustable distance and angle of view [39].
When comparing the two perspectives, it has been observed that the third-person perspective allows users to immediately notice and correct erroneous actions. On the contrary, this real-time feedback is not easily achieved in the first-person perspective due to its restricted field of view. Moreover, this perspective requires users to explore a wider area of the screen and thus use peripheral vision [39].
As a result, the third-person perspective (3PP) is usually the favored one as it tends to provide better outcomes, despite potential drawbacks such as occlusions caused by the participant's own body [38][39].

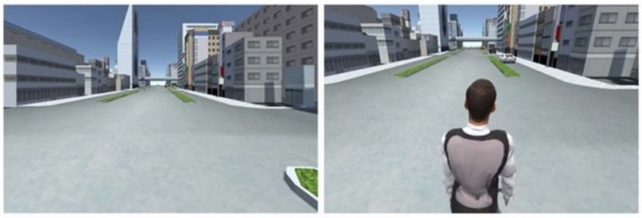

Figure 5: Visual perspectives in virtual reality environments: 1PP on the left, 3PP on the right.

### 2.2.3 VR in stroke rehabilitation

Virtual Reality has been introduced in the rehabilitation context as it is able to offer a controlled and safe learning environment while motivating the patient by adding gaming elements to the exercises [17]. Thanks to Virtual Reality, games can evoke real-life situations and be aimed at helping patients recover capacities for an independent life [40]. An example is reported in the paper of P. Dias and colleagues [40] where the "Enjalbert Test" was used to decide which gestures were relevant for the exercises, and then minigames were developed evoking real-life situations like lifting a barbell, eating an apple or washing dishes. Another example is given by [41] which proposes three games for upper limb assessment: "Pick and Place", in which the user shall pick a solid cube from a table and place it on another one; 'Wall Climbing', where the user is asked to move his/her arm vertically to climb the ladder; "Hit the Ball", where the user moves his/her arm to hit a ball.

**Benefits** The use of virtual reality in post-stroke rehabilitation offers several significant advantages. These include the complete control over the extent of the stimuli, the ability to vary stimuli from simple to more complex ones, the easy assessment and recording of the patient's progress, the creation of a safe learning environment, and the provision of individualized treatments based on the patient's diagnosis and needs[17]. The VR environment encourages the controlled and repetitive execution of exercises, facilitates the analysis of the obtained effects, and significantly boosts patients' motivation by incorporating playful elements into the rehabilitation process [40]. This approach results in improved performance and functionality of the affected limbs, enhanced cognitive functions, stimulated neuroplasticity, and increased autonomy in daily activities [42].

**Limitations** The primary drawback associated with Virtual Reality-based rehabilitation is cybersickness. This term refers to the adverse reactions that some users experience during and after exposure to virtual environments, especially those delivered by highly immersive systems such as HMDs. These adverse effects include symptoms like nausea, visual disturbances, postural instability, headaches, and drowsiness [37]. These could be caused by incongruities in the sensory information received from various sources. The occurrence and severity of these events are influenced by the type of delivery system, as well as the individual user's characteristics

and their ability to manage simulated movements and interactions. Notably, video-display VR systems exhibit minimal presence of these side effects [37].

## 2.3. IMU-based Motion Capture Systems

Motion capture is a technique that involves using both software and hardware to capture human motion and it finds widespread applications in various fields, including entertainment, robotics, medicine and physical rehabilitation [43]. Specifically, IMU-based Motion Capture systems can capture three-dimensional human motion using Inertial Measurement Unit (IMU) sensors, which combine an accelerometer, a magnetometer and a gyroscope [44]:

1. Accelerometers: they measure acceleration in three directions: forward/backward, left/right, and up/down. When the device is not moving, they register the acceleration due to gravity (around 9.81 $m/s^2$). By detecting changes in acceleration, they can tell if the device is moving, how fast it is accelerating and in which direction.
2. Gyroscopes: they measure angular velocity, which means how fast the device is rotating or changing its orientation around three axes: pitch (up and down), roll (tilting side to side), and yaw (turning left or right). Gyroscopes help track changes in orientation and detect rotational movements.
3. Magnetometers: they detect the Earth's magnetic field, which allows the device to determine its absolute orientation with respect to the Earth's magnetic poles. This is useful for finding the device's compass direction or heading.

### 2.3.1 IMU-based MoCap systems in stroke rehabilitation

A crucial aspect of stroke rehabilitation is the capability of monitoring patients' movement in order to provide supervision and evaluation of patients' performance during the rehabilitation process. The information about the patient movement can also be used to provide a feedback to remind the user or the assistive device to adjust the training content or guide a change in posture [18]. For instance, Tsilomitrou et al. [45] presented an application where IMU-based motion capture systems offer real-time feedback to users, enabling the monitoring of training progresses and the creation of personalized training plans by experts. Timmermans et al. [46] devised a technology-supported regimen for task-oriented arm training among stroke patients, employing tracking sensors, an exercise board and a software toolkit to enhance arm performance. IMUs can also provide valuable feedback for controlling external devices during training sessions. As an example, Mittag et al. [47] utilized IMUs for the real-time control of exergames.

**Benefits** IMU-based MoCap systems consist of tiny lightweight components that offer significant advantages, including portability, adaptability, and comfortable wearability, as they can be worn directly on the skin or concealed beneath clothing [28]. Moreover, they require no fixed infrastructure to be used and they are cost-effective. These characteristics make IMU-based Mocap systems suitable for monitoring human motion not only during rehabilitation sessions but also in everyday settings [19].

**Limitations** The IMU-based Mocap system, however, comes with some drawbacks. Firstly, IMU sensors are susceptible to drifts, leading to changes in sensing results over time. Secondly, the method of wearing IMUs can introduce slight positional changes as the skin moves or the device loosens. Lastly, magnetometers within IMUs can be influenced by external magnetic fields, potentially affecting the results' accuracy. To mitigate these issues, different solutions has been suggested, including algorithmic data correction, drift auto-calibration and integration with other systems for more comprehensive measurements [18].

## 2.4. Integrated Full-body Wearable Suit

Integrated devices are gaining prominence in the medical and rehabilitation fields. They consist of full-body suits combining Functional Electrical Stimulation systems and/or Motion Capture systems, offering a comprehensive solution that can be easily used in home settings.
For instance, the Smartsuit Pro II by Rokoko is a motion capture suit equipped with 9 degrees of freedom IMU sensors, enabling precise movement tracking. It allows to engage in a natural and intuitive way with the virtual world, gradually becoming an integral part of the modern daily life. This suit not only serves as a content creation tool but has also found applications in treating children with autism and supporting research in rehabilitation and physical therapy [48].
On the other hand, the Exopulse Mollii Suit by Ottobock integrates multiple FES electrodes designed to stimulate muscle groups in the upper and lower body. It targets pathological conditions like cerebral palsy, multiple sclerosis, stroke and other neurological disorders that affect motor functions. The suit features 58 electrodes

delivering varied and mild impulses to both tense and spastic muscles as well as to the weaker muscles that typically counterbalance them. These impulses promote the relaxation of the more contracted muscles by pre-activating their hypotonic antagonists (reciprocal inhibition). This process restores a portion of the natural mechanism that facilitates smoother movements for the body [20].
Teslasuit by VR Electronics is an example of a device that combines both FES and MoCap systems. Initially designed for immersive gaming, it features a haptic feedback system, an IMU-based MoCap system and a Unity plugin for Virtual Reality. It is now finding applications in the medical and rehabilitation field as a standalone FES device [49].
Galofaro and colleagues [50] introduced an experimental setup aimed at enhancing the virtual reality experience through the use of Teslasuit. This technology was employed to generate, through neuromuscular electrical stimulation (NMES), a haptic sensation of resistance in the antagonistic muscles when interacting with virtual objects in VR. To achieve this, a personalized biomechanical model was developed to estimate the torque exerted at the elbow during object manipulation, facilitating the delivery of appropriate electrical muscle stimulations. Their study conducted experiments to assess the differences among three conditions: NMES-based haptic feedback, physically lifting objects and a condition without the haptic feedback. The outcomes revealed significant distinctions in terms of metabolic consumption and users' perception of fatigue between the conditions involving electrical stimulation and those with real-weight objects compared to the condition without any external load. This suggests that the implemented feedback system effectively replicated interactions with virtual objects, implying its potential applications in diverse domains such as gaming, rehabilitation and educational contexts.
Caserman and colleagues [51] introduced a novel method for assessing human movements using the Teslasuit technology. Their approach involved training probabilistic movement models using data from 10 inertial sensors to identify errors in exercise execution. Furthermore, they incorporated haptic feedback by employing transcutaneous electrical nerve stimulation (TENS) to correct these errors promptly as they occurred during the workout. The study's findings, derived from a dataset collected on fifteen participants, demonstrated the effectiveness of this approach in detecting significant errors in real-time movement execution and in precisely delivering haptic feedback to the corresponding body locations. These results highlight the promising potential of Teslasuit for movement assessment, as it can provide users with valuable haptic feedback to enhance and refine their movements.

# 3. Objectives

This study focuses on the feasibility of using Teslasuit in a Functional Electrical Stimulation induced motion recovery environment. Two main objectives can be distinguished:

1. Teslasuit validation
   1.1 Validation of the motion capture system
   1.2 Validation of the electrical stimulation (ES) system
2. Development of a imitation-based exercise protocol in a virtual environment

The analysis focuses on the upper limb. In particular, point 1.1 aims at validating the angles that describe elbow and shoulder movements, whereas in point 1.2 the performance of the electrical stimulation system is explored.
Once validated the motion capture and the electrical stimulation systems, these are used to develop imitation-based rehabilitation exercises in a Virtual Reality environment.

# 4. Materials and methods

## 4.1. Materials

### 4.1.1 Teslasuit

Teslasuit is a smart textile full-body suit that incorporates advanced technology to provide complete sensory immersion during interaction with virtual environments. Specifically, it was designed to enable users to perceive controlled haptic sensations in order to enhance their gaming experience. Nowadays, Teslasuit wants to expand its applications in the medical field to include areas such as rehabilitation.
The suit consists of a jacket and trousers that come in a range of sizes as well as specially engineered zips, straps, and stretchy hypoallergenic material to suit all body shapes. The suit is shown in Figure 6.
It includes 3 major features:

- **Motion capture module**: uses Inertial Measurement Unit (IMU) sensors, embedded in the suit in fixed place (illustrated in Figure 7a), to track, record and monitor the movements and positioning of the users.

Figure 6: Teslasuit

It also creates a digital representation of the user (an avatar). It can be used for animation creation (e.g. games, movies), performance monitoring and capture (e.g. sports), ergonomics and human factor testing (research, data analysis).

- **Electrical stimulation module**: uses dry textile voltage-controlled electrodes, embedded in the suit in anatomic locations (shown in Figure 7b). Electrodes are paired into channels and each channel refers to a muscle. The electrodes, including both anodes and cathodes, are distributed across channels. Each channel consists of both an anode and a cathode, although certain channels share the same anode. Electrodes can provide Neuromuscular Electrical Stimulation pulses, to induce an artificial muscle contraction, and Transcutaneous Electrical Nerve Stimulation to simulate haptic sensations. Using this system, Teslasuit can provide physical feedback based on the visual simulation that may be experienced in a VR environment.
- **Biometry module**: comprises a photoplethysmography (PPG) that provides information about the user's heartbeat per minute (BPM) and pulse rate variability (PRV). This enables the creation of interactive VR training content that adapts to the participant for customized experiences.

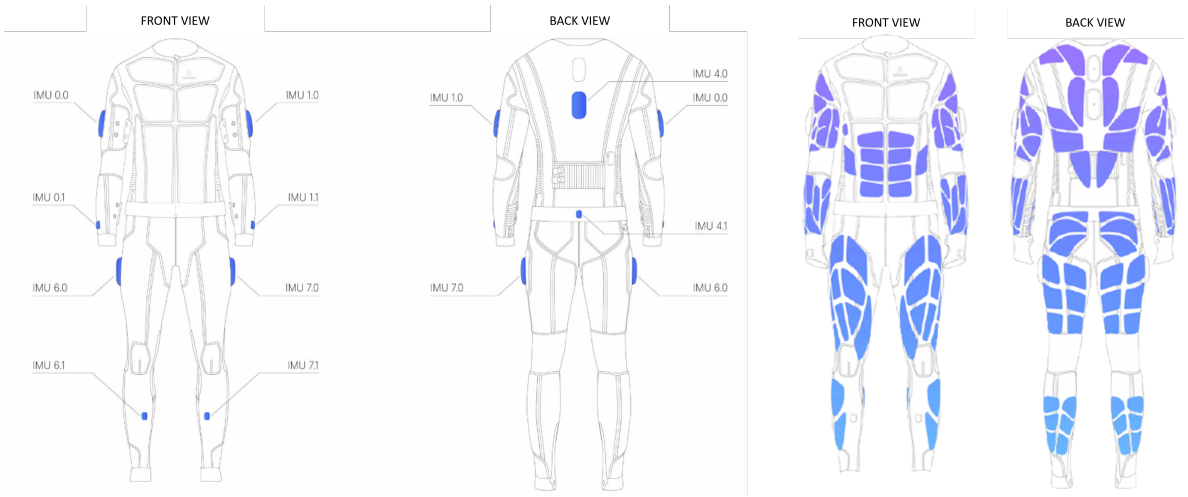


(a) (b)

Figure 7: Teslasuit IMU (7a) and electrodes (7b) position

This study relies on Teslasuit version 4.5.1 medical, size M, male users. "Medical" refers to the additional zippers to facilitate the wearability of the suit. In this version, only MoCap and ES modules are comprised. For the purpose of this study, only the jacket was used.
The technical characteristics are shown in Table 1.

| MOTION CAPTURE MODULE | | ELECTRICAL STIMULATION MODULE | |
|---|---|---|---|
| **Number of IMU** | 10 | **Number of electrodes** | 62 (jacket)<br>52 (trousers) |
| **IMU type** | 9 axis and 6 axis modes | **Number of channels** | 48 (jacket)<br>32 (trousers) |
| **IMU location** | Embedded in the suit in fixed places | **Type of stimulation** | EMS, TENS |
| | | **Electrodes location** | Anatomic locations |
| **IMU frame rate** | 200Hz | **Electrodes location** | Anatomic locations |
| | | **Stimulator circuit** | Voltage controlled |
| **Roll and pitch** | 0.05° | **Frequency range** | 1-300 Hz per channel |
| | | **Voltage range** | 0-55 V AC |
| **Heading** | 0.1° | **Current range** | $\sim$ 50 mA per 1 kOhm |
| | | **Pulse width range** | 1-320 $\mu s$ |

Table 1: Teslasuit technical features [52]

Two software are provided with the suit [49]:

- **Control Center**: it contains the suit API needed to connect the suit and the computer.
  It allows performing the calibration of the electrical stimulation, which consists in setting the minimum and maximum pulse width values for each channel. In particular, this is done by varying the pulse width in a range that goes from 1% to 100% of the suit's full pulse width range (specified in Table 1). The stimulation is provided as a train of impulses with a frequency fixed to 100Hz and a total duration of 1s. Minimum and maximum values set in this phase, are then used as limits for the pulse width range applicable to the specific subject.
- **Studio**: it has 2 modules:
  - Motion capture module: it is used to visualize and record the subject's movements while wearing the suit. When the recording is over, the biomechanical data are available. These data consist of the quaternions referred to the limb's location, the joint angles, velocities and accelerations. They can be directly visualized in the module interface or exported as a *.csv* file.
  - Electrical stimulation module: it is used to create and test haptic sensations. Haptic stimuli can be modified in pulse width of the single impulse, and in duration and frequency of the train of impulses.

Teslasuit is also provided with a **Unity plug-in**. Unity is a software used to develop virtual reality environments. This plug-in reads in real time the data coming from the suit's API (joint angles and limb-referred quaternions) and can control the electrical stimuli delivered by the suit. Consequently, virtual reality interfaces can be developed, allowing the interaction of the subject wearing the suit with the virtual environment.

When using either the Unity plug-in or the motion capture module, it is essential to calibrate the IMU sensors. This is done by asking the subject to stand still in I-Position, with the hand's palm facing the leg, for 2s.

### 4.1.2 Optoelectronic system

In literature, optoelectronic measurement systems (OMS) are often regarded as the gold standard in motion capture. These systems are based on 3 elements:

- Infrared cameras;
- Active or passive markers;
- Data processing software.

In order to determine the three-dimensional location of every marker, a minimum of two cameras is necessary, exploiting the principles of stereo-photogrammetry. Each camera establishes the flat coordinates of the marker's center and subsequently, using camera parameters, the marker's three-dimensional representation is reconstructed. This process mirrors the same concept found in human stereoscopic vision, where our brain receives images of a three-dimensional object in space from both eyes and combines them to create a stereoscopic reconstruction.

Markers are strategically placed on the subject's body to track specific body segments. and thus it is essential for these markers to be highly visible to the cameras. Active markers incorporate LEDs and emit light, enabling precise tracking. However, they require additional cables and batteries that reduce the freedom of movement.

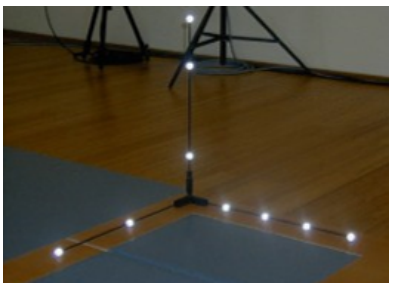

Figure 8: Triad of wands used to set up cameras calibration parameters during static calibration

On the other hand, passive markers are based on reflective surfaces but they may suffer from uneven illumination, making their position recognition more challenging.

The data processing software merges information coming from different cameras and returns the absolute position of the markers at any time.

The calibration of the optoelectronic systems is essential to set up the environment.
This phase consists of two steps:

- Static calibration: a triad (three rods with markers attached to them) is placed in the center of the lab. The system knows the triad dimensions (the distances between the markers) and orientation, therefore it calculates the calibration coefficients of the various cameras so that they correctly acquire the position of the markers in space. The three axes of the triad will be the x y and z, as shown in Figure 8 and they will act as the reference for the position of the markers.
- Dynamic calibration: a wand of known size and with markers placed at a known distance is moved for one minute in space to determine the acquisition "volume", i.e. the cube within which the cameras must correctly recognize the position of the markers even as they move.

Once the calibration is done a file is generated. This can then be reloaded for each acquisition so that the system is ready to acquire correctly. Indeed, if the position of the cameras and the global environment do not change between acquisitions, the same calibration file can be used multiple times.

This study relies on a system based on 8 SMART DX 400 (BTS SPA, IT) cameras with an acquisition frequency of 100Hz.

## 4.2. Acquisition Protocol

Tests were run on subjects that voluntarily accepted to take part in the study and signed a written informed consent.
All of them matched the suit requirements:

- Male
- Healthy and able to perform the designed tasks
- Chest measurement: 96-101cm
- Waist measurement: 84-89cm

All subjects tested in this work were aged between 22-25 years. The study was approved by Ethical Committee of Politecnico di Milano (Nr 13/2021).

### 4.2.1 Motion Capture Validation

The aim of these tests was to evaluate the validity of upper limb angles (shoulder angle of elevation (AOE) and plane of elevation (POE), and elbow flexion-extension (FE)) with respect to the optoelectronic system data, assumed as the gold standard.
This study relies on an optoelectronic system based on 8 SMART DX 400 (BTS SPA, IT) cameras with an acquisition frequency of 100Hz; passive markers and *Smart analyzer* software.
5 healthy subjects (all male, aged 22-25) were acquired in this phase. Acquisitions took place at the Luigi Divieti laboratory of Politecnico di Milano.
The acquisition protocol can be summarized in 4 phases:

1. Markers and Teslasuit set up;
2. Optoelectronic system calibration;

3. Teslasuit motion capture system calibration;
4. Execution of the tasks.

*Phase 1*: In order to capture data with the optolectronic system, 8 passive markers are positioned on the right arm: Right Acromion (RA), Left Acromion (LA), Seventh cervical Vertebra (C7), Medial Epicondyle of the elbow (ME), Lateral Epicondyle of the elbow (LE), Ulnar Styloid (US), Radial Styloid (RS), $2^{nd}$ Metacarpophalangeal joint (2MCP). Marker placement was chosen specifically to allow the 3D reconstruction of the upper limb joint angles [53]. Final positions of the markers are shown in Figure 9.
The Teslasuit setup only requires the user to wear the suit and connect it to its power bank.

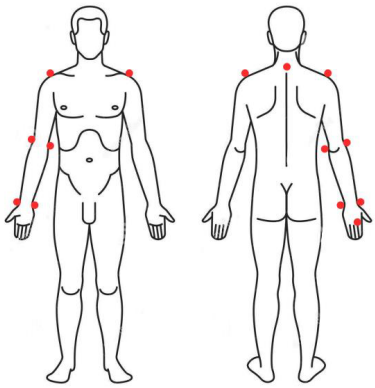

Figure 9: Positions of the markers on the subject

*Phase 2*: Optoelectronic system calibration is performed using the calibration file already generated in the laboratory, assuming that no crucial differences had been made in the acquisition volume and cameras set up.

*Phase 3*: Teslasuit IMU calibration is performed in *Studio* interface, asking the subject to stand still in I-Pose for 2s.

*Phase 4*: 5 different tasks were performed to assess the behavior of both elbow and shoulder angles, that are respectively Flexion Extension angle, and Angle of Elevation and Plane of Elevation angles. The tasks, shown in Figure 10, are:

- *Reach to grasp:* reaching of an object positioned in front of the subject [54];
- *3D pointing:* lateral pointing [55];
- *Hand to nose:* reaching of the subject's nose [56];
- *Shoulder lateral flexion:* shoulder abdo-adduction on the frontal plane;
- *Elbow flexion-extension:* elbow flexion-extension on the sagittal plane.

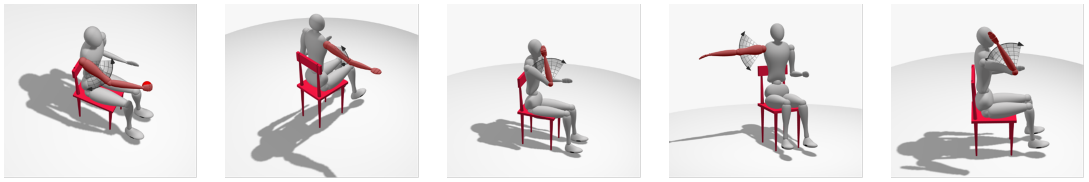

(a) *Reach to grasp* (b) *3D pointing* (c) *Hand to nose* (d) *Shoulder lateral flexion* (e) *Elbow flexion-extension*

Figure 10: Designed tasks for angle validation

Supposing that there is symmetry in the behavior of the two sides for a healthy subject, all the tasks were executed only with the right arm. The initial position consists of sitting in front of a table, then, each task is performed 10 times. Each repetition of *Reach to grasp, 3D pointing,* and *hand to nose* starts with the right hand on the table with the elbow flexed at $\sim 90$ deg; whereas *shoulder lateral flexion* and *elbow flexion-extension* repetitions start with the arms by the sides, palms facing the chair.
Prior to each task, a trigger movement (fast elbow flexion) is made.

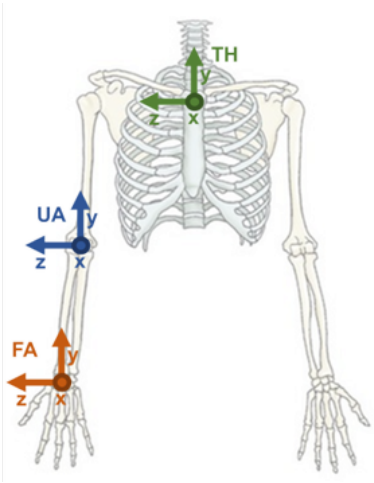


Figure 11: Obtained local reference systems defined according to ISB convention

During the task execution, data are acquired. For the optoelectronic system, data are recorded through the *SMART-Tracker* software with an acquisition frequency of 100Hz. They consist of 3D coordinates representing the positions of markers.
As already mentioned, the Teslasuit software "Studio" enables the recording of the angles' quaternions as well as the biomechanical angles. However, biomechanical angles were not used in this study since they are not defined following the International Society of Biomechanics (ISB) convention.
Hence, while tasks are performed, only quaternions representing the rotation of upper arm, forearm, and thorax with respect to the root bone (Hips) are acquired. This is done through *Studio*, that works at a variable acquisition frequency of around 60Hz. These data are then resampled at 100Hz to be comparable with Smart ones.

Optoelectronic local reference systems result from a protocol developed in the *SMART-Analyzer* software:

1. *Marker interpolation:* in case a marker is not visible for a certain time, the software approximates its trajectory so that the marker output signal exists for the whole acquisition.
2. *Midpoints creation:* lateral markers positions are used to compute midpoint positions for each instant and each joint: ME and LE are used for the elbow one, US and RS for the wrist one, LA and RA for the shoulder one.
3. *Local reference system creation:* 3 reference systems are defined following ISB convention:
   **Upper Arm:** z-axis is directed from ME towards LE, x-axis is perpendicular to the plane defined between z-axis and a vector that goes from the elbow midpoint to RA, y-axis is the result of cross product between x-axis and z-axis, using the elbow midpoint as origin.
   **Forearm:** z-axis is directed from US towards RS, x-axis is perpendicular to the plane defined between z-axis and a vector that goes from the wrist midpoint to LE, y-axis is the result of the cross product between x-axis and z-axis, using the wrist midpoint as the origin.
   **Thorax:** z-axis is the perpendicular bisector between LA and RA, x-axis is perpendicular to the plane defined between z-axis and a vector that goes from the shoulder midpoint to C7, y-axis is the result of the cross product between x-axis and z-axis.
   The 3 resulting reference systems are shown in figure 11
4. Reference system file export: this file contains the local reference system coordinates, which describe changes in the limb position over time.

Teslasuit quaternions and optoelectronic local reference systems are used to construct roto-translation matrices through a Matlab function.
These are then used to obtain AOE, POE, and FE according to International Society of Biomechanics (ISB) convention [57].

Specifically, FE angle, which describes elbow movements. It is defined as the relative angle between the upper arm y-axis ($UA_y$) and the forearm y-axis ($FA_y$):

$$FE = arcos\left(\frac{FA_y \cdot UA_y}{\|FA_y\| * \|UA_y\|}\right) \tag{1}$$

AOE and POE angles describe shoulder movements.

The former is defined as the relative angle between thorax y-axis ($TX_y$) and upper arm y-axis ($UA_y$):

$$AOE = arcos\left(\frac{UA_y \cdot TX_y}{\|UA_y\| * \|TX_y\|}\right) \tag{2}$$

The latter is computed as the relative angle between the thorax z-axis ($TH_z$) and the projection of the upper arm y-axis ($UA_y$) onto the plane defined by the thorax x-axis and z-axis ($TH_{xz}$):

$$POE = sign * arcos\left(\frac{p_{y_{xz}} \cdot TX_z}{\|p_{y_{xz}}\| * \|TX_z\|}\right) \tag{3}$$

FE is defined as positive while flexing, AOE while elevating and POE when moving the arm frontally.
POE is ill-defined when AOE is null because in that case, $UA_y$ is orthogonal to $TH_{xz}$ and thus the projection $p_{y_{xz}}$ is null and Eq. 3 loses its significance.

The Teslasuit angles computation just described is then used in both FES validation and imitation-based protocols.

### 4.2.2 Electrical Stimulation Validation

The aim of these tests was to verify whether the specific Electrical Stimulation channel can induce the expected movement and range of motion. This study analyzed channels referred to: anterior deltoid *(ch0)*, biceps *(ch1)*, posterior deltoid *(ch2)* and triceps *(ch3)*.
5 healthy subjects (all male, aged 22-25) were acquired for this section.
Acquisitions took place at the Neuroengineering and Medical Robotics Laboratory (NEAR LAB) of Politecnico di Milano.

The acquisition and stimulation protocol can be summarized in 4 phases, each one repeated for the right and left arms consequently:

1. Virtual reality avatar calibration;
2. Voluntary execution of the movement;
3. Calibration of the electrical stimulation values;
4. Execution of ES-induced movement.

During each movement, quaternions related to upper body segments are recorded through the Unity interface with a rate of 80Hz.
Quaternions are then used to compute biomechanical angles, as described in the section 4.2.1 . For each stimulation channel, only the angle referred to the expected movement is analyzed: FE angle for biceps and triceps, AOE angle for anterior and posterior deltoid. POE is not taken into consideration due to its poor performance as it will be shown later in the results section.
Apart from the voluntary execution of the movement, the entire protocol is repeated twice: soon after the suit was worn, and again after a 30-minute interval. This is done to evaluate the stimulation repeatability over time. The two sets of acquisition will be referred to as *test 1* and *test 2*.

*Phase 1*: the subject is asked to stand still in I-Pose for 1s.

*Phase 2*: the voluntary movement related to the examined channel (shoulder abduction-adduction for anterior and posterior deltoid, elbow flexion-extension for biceps and triceps) is repeated 5 times. The starting position for each channel is the I-Position, except for triceps in which case the subject is sitting and his arm lays on a support with the forearm hanging and creating a 90deg elbow angle. In this way, the triceps-induced movement is performed anti-gravity.

*Phase 3*: an increasing ramp of pulse width values, going from 0 to 100% of the suit full pulse width range, is provided. Each pulse width value is delivered for $1s$. Minimum and maximum pulse width values are saved: the former is the value at which a muscle contraction is visible, the latter corresponds to the value at which the subject starts to feel pain (pain threshold). When the maximum value is recognized, stimulation stops.

*Phase 4*: the stimulation is provided as an increasing pulse width ramp of 0.5s going from the minimum to the maximum and then the maximum is kept for 2s. Lastly, a 2.5 seconds pause elapses between the end of the

plateau and the start of the following ramp. A total of 5 repetitions is recorded. Stimulation pattern is shown in Figure 12.

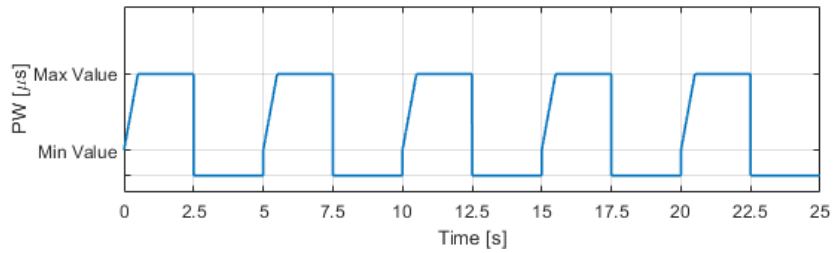


Figure 12: Stimulation pattern in *phase 4*

Both in *phase 3* and *phase 4* the stimulation is provided as a train of pulses with 40Hz frequency.

An interface (illustrated in Figure 13) was developed to guide the subject during data acquisition: this shows in real time which channel (both in terms of muscle and side) is being stimulated, the subject name and which protocol phase is going on.

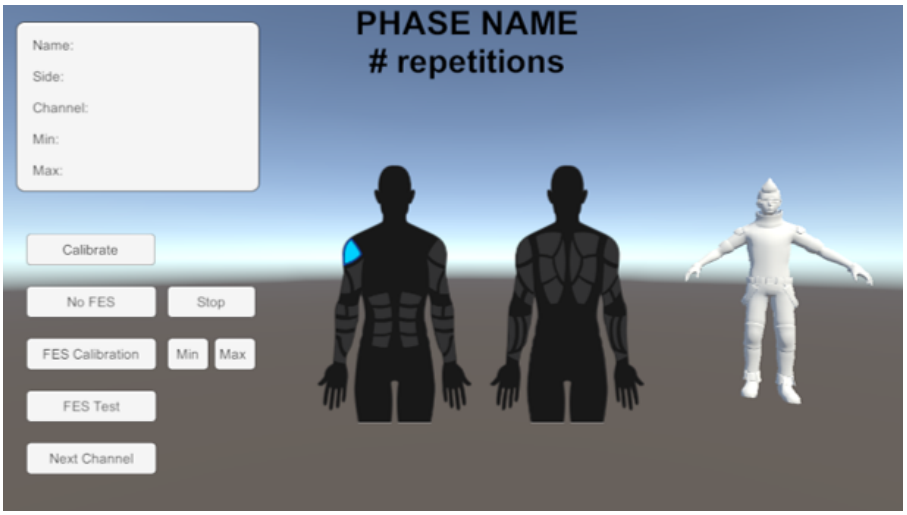


Figure 13: Interface of the FES Validation

### 4.2.3 Imitation-based exercise

Inspired by the concept of Mirror Therapy, the following protocol suggests a series of exercises based on the execution of a movement with one arm (assuming stroke survivors as potential users of this platform, it corresponds to the "healthy" arm). This movement is recorded through the suit and replicated on the other arm (the "impaired" one) using Functional Electrical Stimulation.
The proposed exercises use angles and channels that have been considered valid based on the results of the initial motion capture and ES module validation tests. Specifically, the considered angles are AOE and FE, while the channels of interest are those associated with anterior deltoid, biceps, and triceps.

The exercise implementation methodology can be broken down into 4 specific phases:

- **Acquisition of the target trajectory**: upon pressing the "start" button, the subject is asked to perform a movement with one arm. Meanwhile, AOE and FE are recorded and saved as target trajectories. The recording stops when the subject returns to the initial I-pose position (i.e. both the FE and AOE angles are below a threshold set to 5°).
- **Reconstruction of the target trajectory using a beta-function**: all acquired trajectories are divided into ascending, plateau, and descending phases. The ascent phase begins when the trajectory derivative overcomes 10°/s and terminates at 80% of the trajectory's maximum. From this point on there is the plateau phase which continues until reaching 80% of the maximum along the descending phase. Subsequently, the descent phase follows, ending when the trajectory derivative goes below -10°/s. The

duration of each phase, along with the maximum value of the trajectory, are used to rescale a beta function (a=4, b=4), to be employed in the algorithm as a simplified target trajectory, as shown in figure 14.

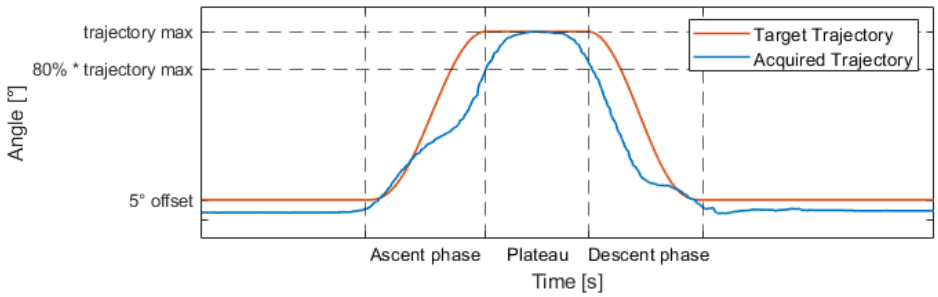


Figure 14: Target trajectory creation starting from the acquired trajectory

Each muscle is linked to its specific target trajectory: the biceps is linked to the elbow flexion trajectory, the anterior deltoid is linked to the shoulder abduction trajectory and the triceps is linked to the elbow extension trajectory. Specifically:

- The elbow flexion trajectory, described by the FE angle, is composed by the ascending phase followed by the maximum plateau.
- The shoulder abduction trajectory, described by the AOE angle, is composed by the ascending phase followed by the maximum plateau and 5% of the descent. This adjustment proved necessary as experimental observations revealed that the position of the maximum was not maintained but an angle decrease was exhibited instead. This led to a significant error between the target and FES-induced trajectory, resulting in a subsequent stimulation pattern characterized by pulse width peaks.
- The elbow extension trajectory, described by the FE angle, is considered just in case of an anti-gravity movement: the trajectory is composed by the maximum plateau (half of the duration belongs to the extension trajectory, the other half to the flexion trajectory) followed by the descending phase and a 150ms plateau at zero, needed to compensate for the muscular delay.

- **Construction of the stimulation pattern**: the ES-induced movement of the other arm is regulated at each repetition with an Iterative Learning Control (ILC) algorithm. This takes as input the error between the target and the ES-induced trajectory acquired during the previous repetition and gives as output the pulse width values to be used in the following repetition.
The error, referring to the k-th repetition is defined as:

$$error^k(i) = \theta^k_{target}(i) - \theta^k_{acquired}(i) \tag{4}$$

where $i$ identifies the time frame and goes from 0 to the length of the target trajectory. This error is used to adjust the pulse width value for each frame of the following k+1 repetition:

$$PW^{k+1} = PW_{min} + \frac{PW_{max} - PW_{min}}{ROM} * \bar{u}^{k+1} \tag{5}$$

$$\bar{u}^{k+1} = \bar{u}^k + \lambda * \bar{Q} * \bar{error}^k \tag{6}$$

where $\lambda$ is an adimensional scalar learning gain (set to 0.2) and $Q$ is a 1x9 smoothing filter. The $\lambda$ gain, set to 0.2, adjusts how quickly the algorithm learns and adapts during subsequent iterations, while the Q-filter improves the algorithm's robustness, smoothing out the control signal.
The ILC algorithm is involved only during anti-gravity movements (elbow flexion, anti-gravity elbow extension, shoulder abduction). Gravity-assisted movements (gravity-assisted elbow extension, shoulder adduction), instead, are simply accompanied by a descending pulse width ramp, that goes from the last value of pulse width given as output from the ILC to the subject minimum value.
The obtained PW values are anticipated of 375ms to correct the muscular and system response delay observed during experiments and to enhance the time synchronization between the target trajectory and the response one.
- **Stimulation and acquisition of the ES-induced trajectory**: the subject receives the stimulation defined by the ILC algorithm while the ES-induced trajectory is acquired to compute the tracking error.

A pause of 1.25 seconds is given between two subsequent stimulation patterns. Figure 15 shows how the stimulation is performed. The stimulation is always delivered as a train of pulses with a 40Hz frequency.

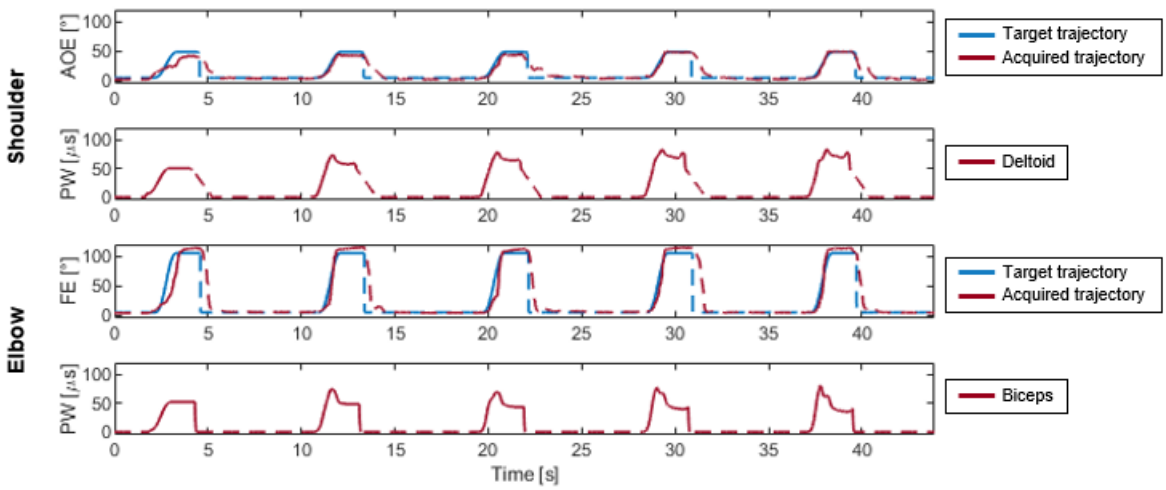


(a) *Hand to mouth: self selected speed*
*Subject 3*

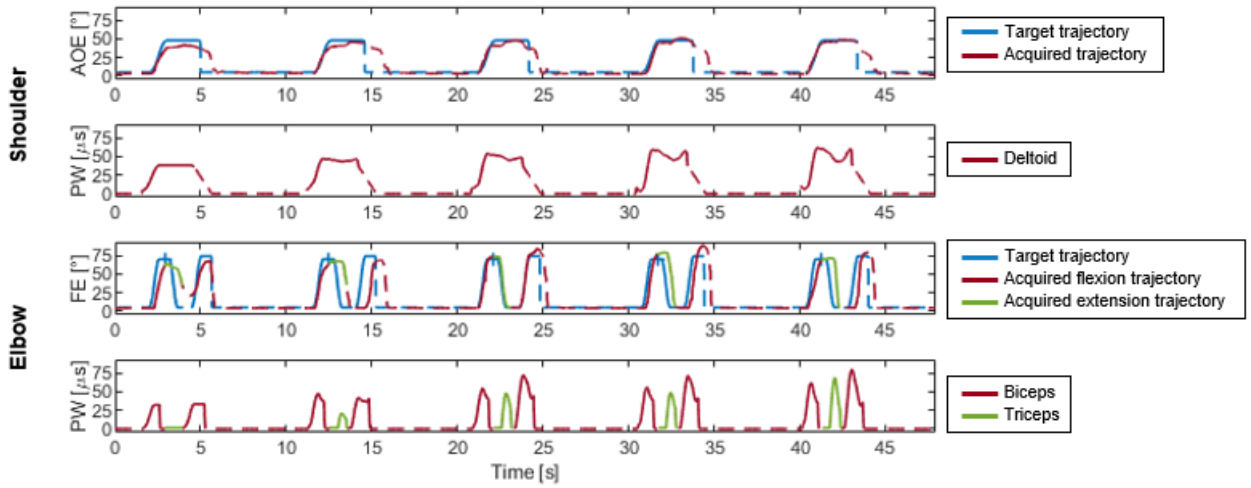


(b) *Lateral reaching: wide movement*
*Subject 4*

Figure 15: Stimulation pattern in imitation-based protocol. The solid line represents the controlled trajectory while the dashed line is the uncontrolled one. The vertical blue dash on the target trajectory (in Figure 15b) distinguishes between biceps and triceps action

Regarding the imitation-based exercise protocol, 5 subjects were acquired. Acquisitions took place at the Neuroengineering and Medical Robotics Laboratory of Politecnico di Milano.
This protocol can be summarized in 3 phases:

1. Virtual reality avatar calibration;
2. Calibration of ES values and Computation of ES-induced Range of Motion (ROM);
3. Execution of VR-based exercises

During the execution of the exercise, quaternions related to upper body segments are recorded through the Unity interface as in 4.2.2.

*Phase 1*: calibration of the avatar as it is explained in Section 4.2.2.

*Phase 2*: the calibration of ES values consists in the delivery of the increasing ramp of pulse width values described in Section 4.2.2, while the maximum ES-induced ROM is computed as the joint angle described by

the stimulated limb when the subject maximum PW value is delivered.

*Phase 3*: subjects are asked to perform movements in two 3PP perspective virtual environments, each one with two interaction modalities with objects, resulting in a total of four exercises. Each exercise starts from the I-pose, the subject is asked to voluntarily perform the scene-specific movement once with one arm and then to stay passive and let the other arm execute the movement through the FES-induced contractions for a total of 15 repetitions.
Two virtual environments were developed in this study and are presented in Figure 16:

1. **Kitchen scene** (Figure 16b): the subject is asked to perform a *hand to mouth* exercise by "grabbing" one mug on a table in front of him and bringing it to his mouth. Two velocities of interaction are tested: *self-selected speed*, and *slow speed*, which takes approximately 5 seconds. This kind of movement only involves the biceps and deltoid, hence triceps are not considered.
2. **Supermarket scene** (Figure 16a): the subject is asked to perform a *lateral reaching* exercise by grabbing a target object on a lateral shelf. Two different movement heights are tested by using two targets placed at different heights: a bottle of milk on a higher shelf (*wide movement*) and a cereal carton on a lower shelf (*small movement*). Both modalities of this exercise involve the biceps and the anterior deltoid muscle, the *high lateral reaching* also involves the triceps, during the anti-gravity extension of the elbow.

Since the test was conducted on healthy subjects, in order to prevent muscle fatigue, participants are asked to perform the first repetition with their left arm in the kitchen scene and with the right one in the supermarket scene.

(a) (b)

Figure 16: VR environments developed for the imitation-based exercise protocol

## 4.3. Data Analysis

### 4.3.1 Motion Capture Validation

For every task acquisition, Teslasuit and Smart data are synchronized and segmented in their respective 10 repetitions.
Each repetition is evaluated using ROM and Root Mean Square Error (RMSE).

The Range Of Motion of AOE, POE and FE is calculated as in Eq. 7:

$$ROM_k = max_k - min_k \tag{7}$$

where k is the index of the repetition of the analyzed task.

The RMSE is evaluated only for those angles considered significant in the specific task execution, that is if their optoelectronic ROM is bigger than 15 deg. It is defined as:

$$RMSE_k = \sqrt{\frac{\sum_{i=1}^{n}(otpoelectronic\ data_i - teslasuit\ data_i)^2}{n}} \tag{8}$$

where k is the repetition index of the analyzed task and i is the analyzed time instant of the repetition, that goes from 0 to the length of the repetition.

Eventually, all the $RMSE_k$ of a task are averaged, resulting in a unique value for each subject for each task (Eq. 9):

$$RMSE_s = \frac{\sum_{k=1}^{10} RMSE_k}{10} \tag{9}$$

where s, identifies the subject.

Finally, the Bland Altman plot is computed. It is built putting together all users and all tasks in which the angle is considered relevant, according to the criteria mentioned above.

### 4.3.2 Electrical Stimulation Validation

Each acquisition is segmented into its 5 repetitions, for each repetition the used evaluation metrics are percentage ROM and pulse width integral over time.
The percentage ROM is computed as the ratio between the ROM of ES-induced movements and the one of voluntary movements (Eq. 10).

$$ROM_{\%} = \frac{ROM_{FES}}{ROM_{NO\ FES}} * 100 \tag{10}$$

The integral of the pulse width over time is used as an indicator of the charge administered to the subjects. Specifically, to assess if possible changes in ROM between test 1 and test 2 are due to changes in the provided charge. This metric is computed as follows:

$$\int_t^{t+2.5} PW(t)\ dt = 2.5 * PW_{min} + \frac{4.5 * (PW_{max} - PW_{min})}{2} \tag{11}$$

Lastly, for both metrics, the median values across the 5 repetitions, calculated for all subjects, are compared between test 1 and test 2 by means of Wilcoxon signed-rank test. In the test input data, left and right arm acquisition are considered separately, resulting in 24 different samples both for test 1 and test 2.

### 4.3.3 Imitation-based exercise

To assess the performance of the ILC algorithm controlling the electrical stimulation, the study considered both the RMSE and the End point error (EPE) for each subject and for every repetition of each exercise.
Each test is segmented in its 15 repetitions and then 2 metrics are computed as follows:

- Root Mean Square Error:

$$RMSE = \sqrt{\frac{\sum_{i=1}^{n}(target\ trajectory_i - acquired\ trajectory_i)^2}{n}} \tag{12}$$

  where $i$ refers to the frame of the analyzed iteration whereas $n$ is the length of the target trajectory.
- End-point Error:

$$EPE = target\ trajectory_{MAX} - acquired\ trajectory_{MAX} \tag{13}$$

  where $\max acquired\ trajectory$ is defined as the mean of the values of the acquired trajectory plateau phase.

The median of both these metrics was then extracted over the 5 subjects, obtaining one value for each iteration of each exercise.

## 5. Results and Discussion

In this section, the results of the data analysis are shown and discussed.

## 5.1. Motion Capture Validation

Table 2 shows the obtained RMSE for each task, only for the angles considered involved in the task, compared to their target ROM.

| | Reach to grasp | | 3D Pointing | | Hand to nose | | Shoulder lateral flexion | | Elbow flexion extension | |
|---|---|---|---|---|---|---|---|---|---|---|
| | RMSE[°] Median (IQR) | ROM Target [°] | RMSE[°] Median (IQR) | ROM Target [°] | RMSE[°] Median (IQR) | ROM Target [°] | RMSE[°] Median (IQR) | ROM Target [°] | RMSE[°] Median (IQR) | ROM Target [°] |
| **AOE** | 6.1 (0,9) | 18.6 | 3.8 (15.9) | 55.4 | - | - | 5.5 (2.1) | 66.3 | - | - |
| **POE** | - | - | 26.6 (32.7) | 24.7 | - | - | - | - | - | - |
| **FE** | 4.8 (1,9) | 29.8 | 5.9 (1.5) | 59.7 | 8.0 (4.3) | 58.1 | - | - | 6.6 (3.2) | 103.7 |

Table 2: Angle validation results: median and interquartile range (IQR) values between subjects for each task

The overall results show good performances for AOE and FE, with respectively a median RMSE of 5.5° (1.7°) (target ROM: $\sim$ 55.4) and 6.2° (1.9°) (target ROM: $\sim$ 58.9). In both cases there is an approximately 10% deviation from the reference ROM.
POE is evaluated only for the *3D pointing* task where its median RMSE is 26,6° (32,7°) (target ROM: 24,7°). This poor outcome is due to problems faced during its computation: tasks were not designed to assess POE variations during movement executions, therefore POE could not be validated and, as a consequence, it was not used in further exercises of this work.

Figure 17, shows the Bland Altman plot. Regarding AOE and FE, data largely fall within a confidence interval with a width of about 40°, almost centered around 0. However, this same trend is not observed in POE data, which, as anticipated, display a greater variability.

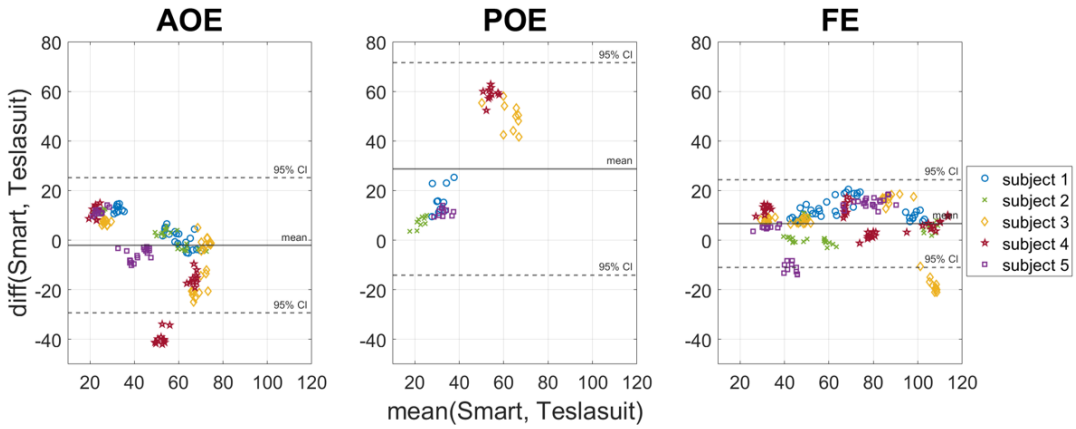


Figure 17: Results of Angle Validation tests: Bland-Altman plots showing the measurement error between the Teslasuit motion capture system and the optoelectronic system for the 3 DOFs

## 5.2. Electrical Stimulation Validation

Figure 18 shows the results in terms of ROM percentage and PW integral over time, highlighting the differences between subjects, limb side and tests.

Regarding the pulse width integral, a relevant variability among subjects in all channels for both tests was noticed. No significant differences or specific trends were observed between Test 1 and Test 2; this behavior is particularly evident in the channels associated with the biceps and triceps.

Considering the percentage ROM, excellent performance was observed in the channels associated with the biceps and triceps, with values very close to 100%. The anterior deltoid also demonstrated good execution but with greater variability among subjects.
The channel linked to the posterior deltoid, despite showing less variability, was the one with the poorest performance, likely due to electrode placement on the suit.

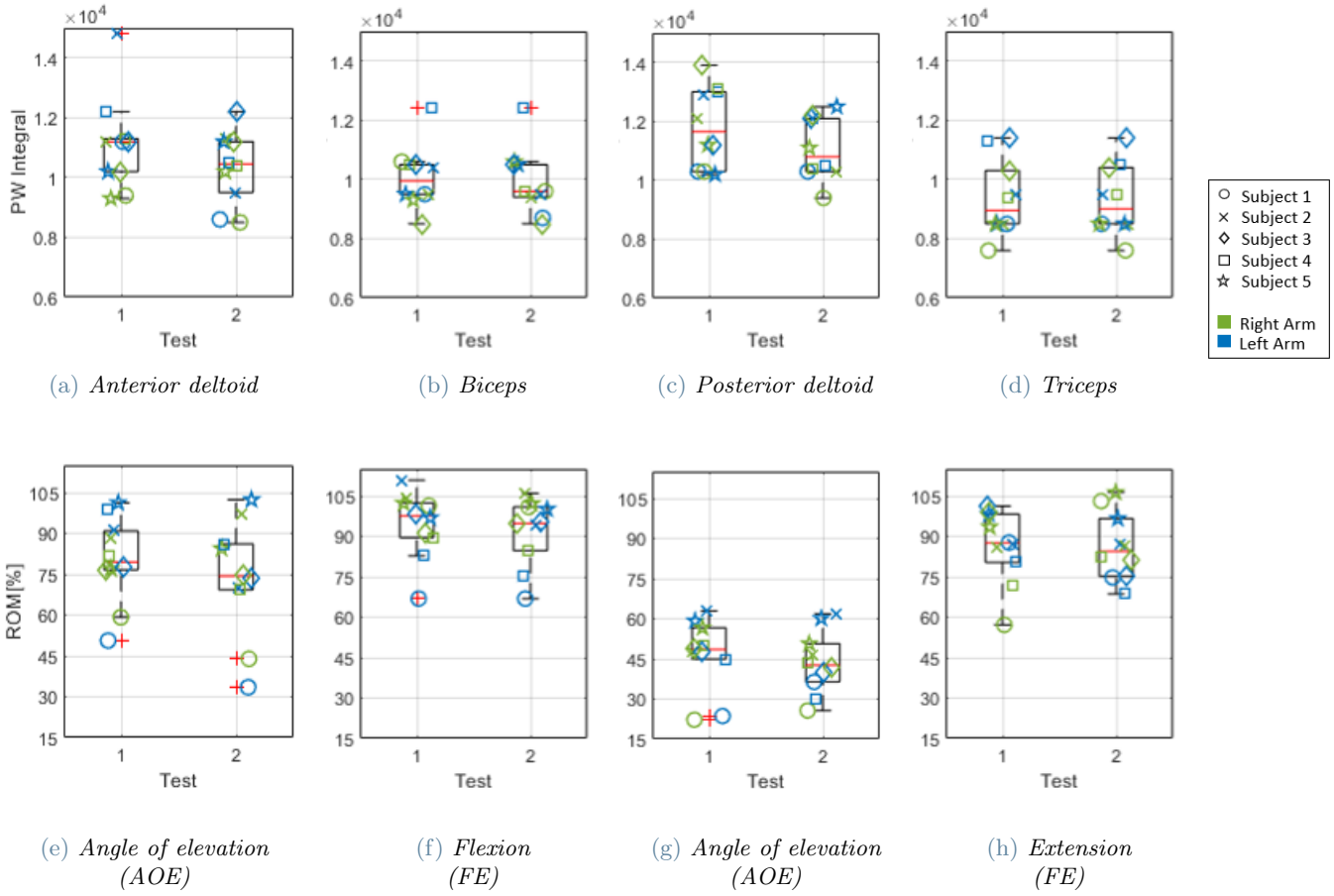


(a) *Anterior deltoid* (b) *Biceps* (c) *Posterior deltoid* (d) *Triceps*

(e) *Angle of elevation (AOE)* (f) *Flexion (FE)* (g) *Angle of elevation (AOE)* (h) *Extension (FE)*

Figure 18: Results of the FES validation tests: the top panels report the integral of the PW provided to each stimulated muscle, while the bottom panels show the ROM of the resulting movement

In all channels, statical analysis found no significant differences between Test 1 and Test 2. Looking at the plots in Figure 18, only a slight trend toward a decrease in performance from test 1 to Test 2 can be noticed, probably associated with muscle fatigue.

## 5.3. Imitation-based exercise

By looking at Figure 19 we can notice a general enhancement in the movement performance around the fifth repetition of each exercise, followed by a subsequent deterioration in the final repetitions, most likely associated with muscle fatigue.
The only exception to this trend is subject 1 whose biceps performances worsen over time, probably due to the fact that the subject's muscles had a tendency to tire rapidly.

Table 3 and Table 4 summarize algorithm performances. They report the median and IQR value computed over the 15 repetitions for the RMSE and the EPE respectively. The value of the single repetition corresponds to the median value over 5 subjects of that specific repetition.

Analyzing the table, an excellent performance can be observed in the AOE, with its median value consistently below 10° for all tasks.
The flexion angle associated with the biceps also exhibits a good performance, with RMSE values all below 20°. Both angles also maintain a limited variability across repetitions.
The extension angle associated with the triceps, instead, exhibits the poorest performance, both in terms of error and variability among repetitions. This is likely due to the fact that flexion and extension movements are referred to the same trajectory but to different muscles, hence any error coming from the stimulation of the biceps consequently affects the stimulation-induced trajectory and the error associated with the triceps.
The results obtained for RMSE and EPE are consistent as Figure 20 illustrates.

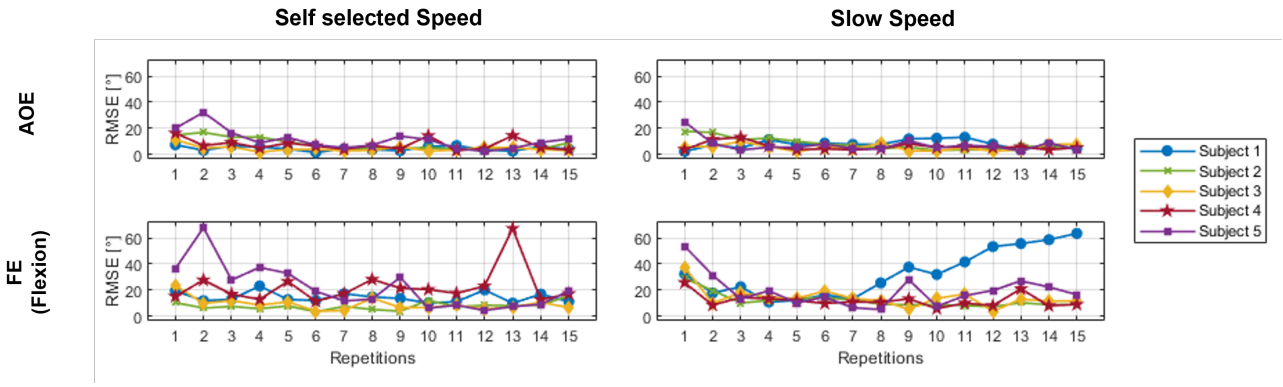


(a) *RMSE Hand to mouth*

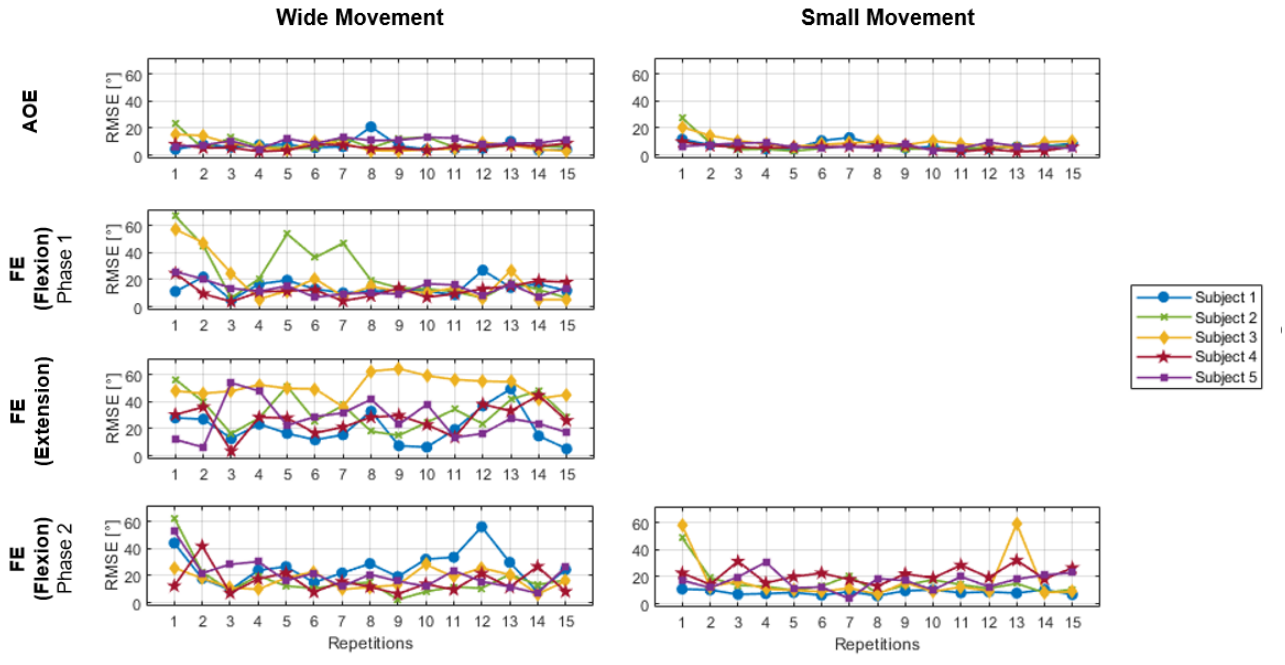


(b) *RMSE Lateral reaching*

Figure 19: Performace of the ILC control algorithm: RMSE evaluated between the target and the actual angle of the two different exercises.

| | | **Angle of elevation (AOE)** | **Flexion (FE)** | | **Extension (FE)** |
|---|---|---|---|---|---|
| | | | **Phase 1** | **Phase 2** | |
| | | Median (IQR) [°] | Median (IQR) [°] | Median (IQR) [°] | Median (IQR) [°] |
| **Hand to mouth** | Self selected speed | 5.10 (2.27) | 11.76 (3.19) | - | - |
| | Slow speed | 5.68 (2.65) | 13.16 (3.89) | - | - |
| **Lateral Reaching** | Small movement | 6.18 (1.20) | 12.35 (4.79) | - | - |
| | Wide movement | 6.43 (2.27) | 11.77 (3.62) | 16.82 (6.86) | 28.53 (10.32) |

Table 3: Performace of the control algorithm: median RMSE between the target and the actual angle of the two different exercise among all the repetitions.

## 6. Conclusions

This study has successfully demonstrated the potential utilization of the Teslasuit as a supportive tool in neuromotor rehabilitation. Initially, the study assessed the reliability of the motion capture system integrated into the Teslasuit, revealing a high level of accuracy in calculating AOE and FE measurements when compared to the gold standard system (i.e., the optoelectronic one). However, further investigation is needed to assess its accuracy in POE calculations.

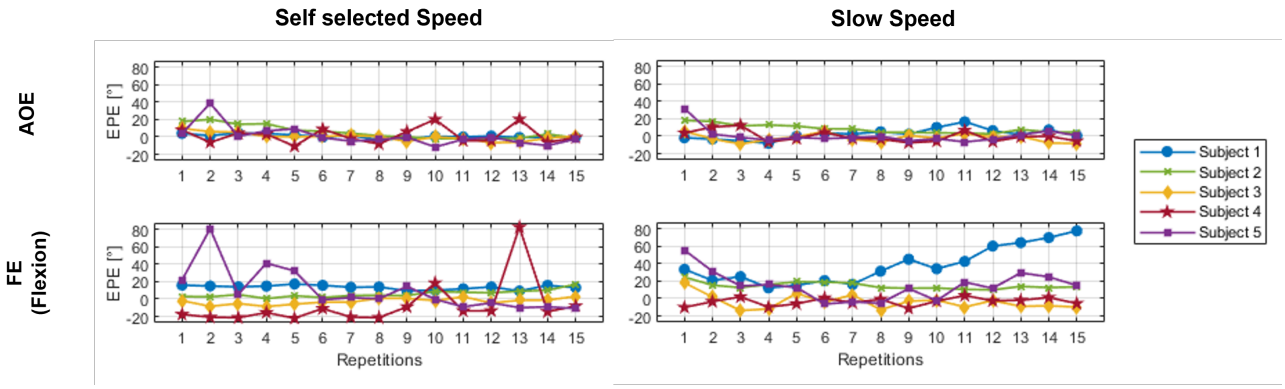


(a) *EPE Hand to mouth*

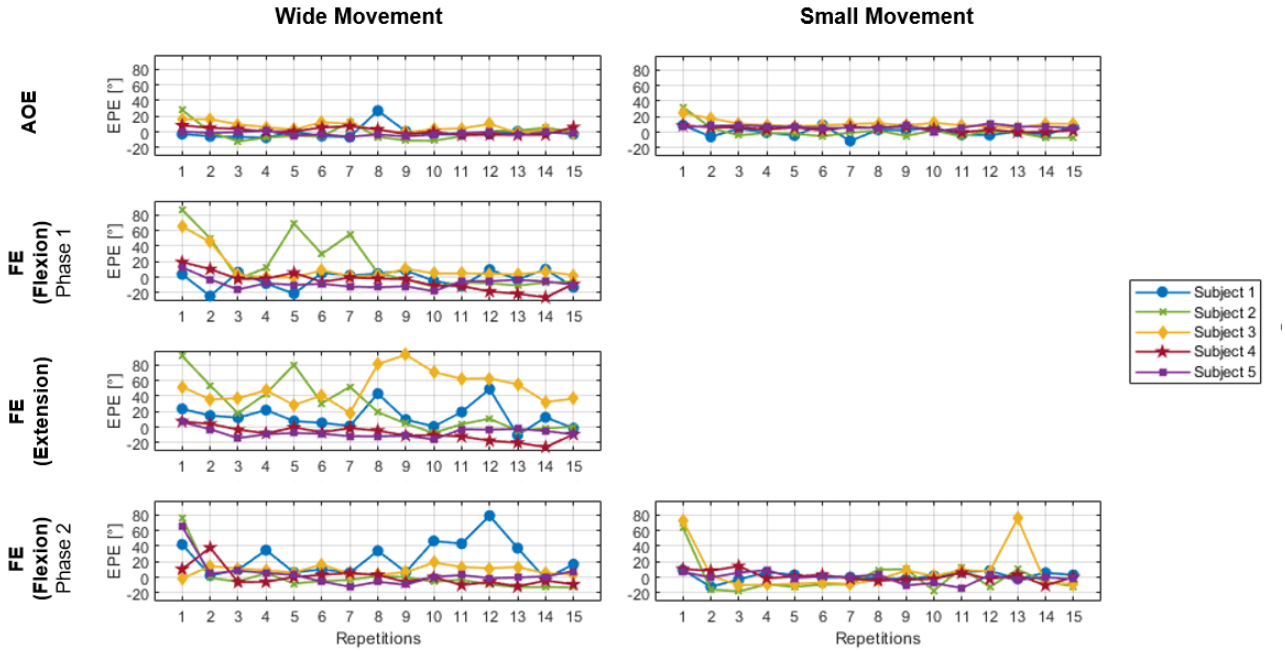


(b) *EPE Lateral reaching*

Figure 20: Performace of the ILC control algorithm: EPE evaluated between the target and the actual angle of the two different exercises.

| | | **Angle of elevation (AOE)** | **Flexion (FE)** | | **Extension (FE)** |
|---|---|---|---|---|---|
| | | | **Phase 1** | **Phase 2** | |
| | | Median (IQR) [°] | Median (IQR) [°] | Median (IQR) [°] | Median (IQR) [°] |
| **Hand to mouth** | Self selected speed | 0.018 (5.04) | 2.59 (3.38) | - | - |
| | Slow speed | 0.56 (4.39) | 12.22 (7.39) | - | - |
| **Lateral Reaching** | Small movement | 5.52 (2.54) | -1.17 (4.50) | - | - |
| | Wide movement | -0.047 (3.02) | -2.24 (7.18) | 2.99 (4.36) | 5.45 (14.77) |

Table 4: Performace of the control algorithm: median EPE between the target and the actual angle of the two different exercise among all the repetitions.

Furthermore, the effectiveness of the electrical stimulation system within the Teslasuit was also established. The ROM achieved through electrically stimulated movements closely resembled the one of voluntary movements, with the exception of the posterior deltoid channel.
Once demonstrated the reliability of Teslasuit features, the study proceeded to develop a VR-based rehabilitative exercise program tailored for post-stroke patients. This program offers various scenarios that can be adapted for being used in diverse settings.
In conclusion, this research highlights Teslasuit's promising role as a comprehensive tool for post-stroke rehabilitation, offering the potential to improve patients' physical performance and quality of life. By combining

FES, Mirror Therapy, and VR within a user-friendly full-body suit, Teslasuit represents a promising tool in the stroke rehabilitation technology, potentially bridging the gap between medical and domestic settings and enabling better recovery prospects for stroke survivors.

## References


[1] What is a stroke?, 1999.

[2] Hatem A Wafa, Charles DA Wolfe, Eva Emmett, Gregory A Roth, Catherine O Johnson, and Yanzhong Wang. Burden of stroke in europe: thirty-year projections of incidence, prevalence, deaths, and disability-adjusted life years. *Stroke*, 51(8):2418–2427, 2020.

[3] Samar M Hatem, Geoffroy Saussez, Margaux Della Faille, Vincent Prist, Xue Zhang, Delphine Dispa, and Yannick Bleyenheuft. Rehabilitation of motor function after stroke: a multiple systematic review focused on techniques to stimulate upper extremity recovery. *Frontiers in human neuroscience*, 10:442, 2016.

[4] Gert Kwakkel, Boudewijn J Kollen, Jeroen van der Grond, and Arie JH Prevo. Probability of regaining dexterity in the flaccid upper limb: impact of severity of paresis and time since onset in acute stroke. *Stroke*, 34(9):2181–2186, 2003.

[5] Dorcas BC Gandhi, Albert Sterba, Himani Khatter, and Jeyaraj D Pandian. Mirror therapy in stroke rehabilitation: current perspectives. *Therapeutics and clinical risk management*, pages 75–85, 2020.

[6] Naoyuki Takeuchi, Shin-Ichi Izumi, et al. Rehabilitation with poststroke motor recovery: a review with a focus on neural plasticity. *Stroke research and treatment*, 2013, 2013.

[7] Belén Rubio Ballester, Martina Maier, Rosa María San Segundo Mozo, Victoria Castañeda, Armin Duff, and Paul F MJ Verschure. Counteracting learned non-use in chronic stroke patients with reinforcement-induced movement therapy. *Journal of neuroengineering and rehabilitation*, 13(1):1–15, 2016.

[8] Ameen Barghi, Jane B Allendorfer, Edward Taub, Brent Womble, Jarrod M Hicks, Gitendra Uswatte, Jerzy P Szaflarski, and Victor W Mark. Phase ii randomized controlled trial of constraint-induced movement therapy in multiple sclerosis. part 2: effect on white matter integrity. *Neurorehabilitation and neural repair*, 32(3):233–241, 2018.

[9] Lynne V Gauthier, Edward Taub, Christi Perkins, Magdalene Ortmann, Victor W Mark, and Gitendra Uswatte. Remodeling the brain: plastic structural brain changes produced by different motor therapies after stroke. *Stroke*, 39(5):1520–1525, 2008.

[10] Joachim Liepert. Evidence-based therapies for upper extremity dysfunction. *Current Opinion in Neurology*, 23(6):678–682, dec 2010.

[11] Dong Wang, Junlu Xiang, Ying He, Min Yuan, Li Dong, Zhenli Ye, and Wei Mao. The mechanism and clinical application of constraint-induced movement therapy in stroke rehabilitation. *Frontiers in Behavioral Neuroscience*, 16, jun 2022.

[12] Leah Daniel, Whitney Howard, Danielle Braun, and Stephen J. Page. Opinions of constraint-induced movement therapy among therapists in southwestern ohio. *Topics in Stroke Rehabilitation*, 19(3):268–275, may 2012.

[13] Myung Mo Lee, Hwi young Cho, and Chang Ho Song. The mirror therapy program enhances upper-limb motor recovery and motor function in acute stroke patients. *American Journal of Physical Medicine &amp Rehabilitation*, 91(8):689–700, aug 2012.

[14] Stefano Masiero, Patrizia Poli, Giulio Rosati, Damiano Zanotto, Marco Iosa, Sefano Paolucci, and Giovanni Morone. The value of robotic systems in stroke rehabilitation. *Expert Review of Medical Devices*, 11(2):187–198, jan 2014.

[15] Cesar Marquez-Chin and Milos R Popovic. Functional electrical stimulation therapy for restoration of motor function after spinal cord injury and stroke: a review. *Biomedical engineering online*, 19(1):1–25, 2020.

[16] Owen A. Howlett, Natasha A. Lannin, Louise Ada, and Carol McKinstry. Functional electrical stimulation improves activity after stroke: A systematic review with meta-analysis. *Archives of Physical Medicine and Rehabilitation*, 96(5):934–943, may 2015.

[17] Matijević Valentina, Šečić Ana, Mašić Valentina, Šunić Martina, Kolak Željka, and Znika Mateja. Virtual reality in rehabilitation and therapy. *Acta Clinica Croatica*, 52(4.):453–457, 2013.

[18] Chenyu Gu, Weicong Lin, Xinyi He, Lei Zhang, and Mingming Zhang. IMU-based motion capture system for rehabilitation applications: A systematic review. *Biomimetic Intelligence and Robotics*, 3(2):100097, jun 2023.

[19] Annick A. A. Timmermans, Henk A. M. Seelen, Richard P. J. Geers, Privender K. Saini, Stefan Winter, Juergen te Vrugt, and Herman Kingma. Sensor-based arm skill training in chronic stroke patients: Results on treatment outcome, patient motivation, and system usability. *IEEE Transactions on Neural Systems and Rehabilitation Engineering*, 18(3):284–292, jun 2010.

[20] Exopulse mollii suit, 1999.

[21] P. Hunter Peckham and Jayme S. Knutson. Functional electrical stimulation for neuromuscular applications. *Annual Review of Biomedical Engineering*, 7(1):327–360, aug 2005.

[22] Dario Farina, Andrea Blanchietti, Marco Pozzo, and Roberto Merletti. M-wave properties during progressive motor unit activation by transcutaneous stimulation. *Journal of Applied Physiology*, 97(2):545–555, aug 2004.

[23] J Thomas Mortimer. Motor prostheses. *Comprehensive Physiology*, pages 155–187, 2011.

[24] Carlo Albino Frigo. *Dispense di Riabilitazione Motoria*. 2019.

[25] Giorgio Sandrini, Volker Homberg, Leopold Saltuari, Nicola Smania, Alessandra Pedrocchi, et al. *Advanced technologies for the rehabilitation of gait and balance disorders*, volume 19. Springer, 2018.

[26] Cesar Marquez-Chin and Milos R. Popovic. Functional electrical stimulation therapy for restoration of motor function after spinal cord injury and stroke: a review. *BioMedical Engineering OnLine*, 19(1), may 2020.

[27] Tadej Bajd and Marko Munih. Basic functional electrical stimulation (FES) of extremities: An engineer's view. *Technology and Health Care*, 18(4-5):361–369, nov 2010.

[28] Trisha M Kesar, Ramu Perumal, Angela Jancosko, Darcy S Reisman, Katherine S Rudolph, Jill S Higginson, and Stuart A Binder-Macleod. Novel patterns of functional electrical stimulation have an immediate effect on dorsiflexor muscle function during gait for people poststroke. *Physical therapy*, 90(1):55–66, 2010.

[29] David N Rushton. Functional electrical stimulation and rehabilitation—an hypothesis. *Medical engineering & physics*, 25(1):75–78, 2003.

[30] Barbara M Doucet, Amy Lam, and Lisa Griffin. Neuromuscular electrical stimulation for skeletal muscle function. *The Yale journal of biology and medicine*, 85(2):201, 2012.

[31] Christian Dohle, Judith Püllen, Antje Nakaten, Jutta Küst, Christian Rietz, and Hans Karbe. Mirror therapy promotes recovery from severe hemiparesis: a randomized controlled trial. *Neurorehabilitation and neural repair*, 23(3):209–217, 2009.

[32] Holm Thieme, Nadine Morkisch, Jan Mehrholz, Marcus Pohl, Johann Behrens, Bernhard Borgetto, and Christian Dohle. Mirror therapy for improving motor function after stroke. *Cochrane Database of Systematic Reviews*, 2018(7), jul 2018.

[33] Dorcas BC Gandhi, Albert Sterba, Himani Khatter, and Jeyaraj D Pandian. &ltp&gt$$mirror therapy in stroke rehabilitation: Current perspectives&lt$$/p&gt$$. *Therapeutics and Clinical Risk Management*, Volume 16:75–85, feb 2020.

[34] Ching-Yi Wu, Pai-Chuan Huang, Yu-Ting Chen, Keh-Chung Lin, and Hsiu-Wen Yang. Effects of mirror therapy on motor and sensory recovery in chronic stroke: A randomized controlled trial. *Archives of Physical Medicine and Rehabilitation*, 94(6):1023–1030, jun 2013.

[35] Jin-Young Park, Moonyoung Chang, Kyeong-Mi Kim, and Hee-Jung Kim. The effect of mirror therapy on upper-extremity function and activities of daily living in stroke patients. *Journal of Physical Therapy Science*, 27(6):1681–1683, 2015.

[36] Lawrence M Parsons, John DE Gabrieli, Elizabeth A Phelps, and Michael S Gazzaniga. Cerebrally lateralized mental representations of hand shape and movement. *Journal of Neuroscience*, 18(16):6539–6548, 1998.

[37] Patrice L Weiss, Rachel Kizony, Uri Feintuch, Noomi Katz, et al. Virtual reality in neurorehabilitation. *Textbook of neural repair and rehabilitation*, 51(8):182–97, 2006.

[38] P Salamin, T Tadi, O Blanke, F Vexo, and D Thalmann. Quantifying effects of exposure to the third and first-person perspectives in virtual-reality-based training. *IEEE Transactions on Learning Technologies*, 3(3):272–276, jul 2010.

[39] Juan Trelles Trabucco, Andrea Rottigni, Marco Cavallo, Daniel Bailey, James Patton, and G. Elisabeta Marai. User perspective and higher cognitive task-loads influence movement and performance in immersive training environments. *BMC Biomedical Engineering*, 1(1), aug 2019.

[40] Paulo Dias, Ricardo Silva, Paula Amorim, Jorge Lains, Eulalia Roque, Ines Serodio Fatima Pereira, Fatima Pereira, and Beatriz Sousa Santos. Using virtual reality to increase motivation in poststroke rehabilitation. *IEEE Computer Graphics and Applications*, 39(1):64–70, jan 2019.

[41] Kai Liang Lew, Kok Swee Sim, Shing Chiang Tan, and Fazly Salleh Abas. Virtual reality post stroke upper limb assessment using unreal engine 4. *Engineering Letters*, 29(4), 2021.

[42] Afsoon Asadzadeh, Taha Samad-Soltani, Zahra Salahzadeh, and Peyman Rezaei-Hachesu. Effectiveness of virtual reality-based exercise therapy in rehabilitation: A scoping review. *Informatics in Medicine Unlocked*, 24:100562, 2021.

[43] Ricardo Tobon. *The Mocap Book: A Practical Guide to the Art of Motion Capture*. Foris Force, 2010.

[44] Manuela Galli. *Valutazione Funzionale*. 2019.

[45] Ourania Tsilomitrou, Konstantinos Gkountas, Nikolaos Evangeliou, and Evangelos Dermatas. Wireless motion capture system for upper limb rehabilitation. *Applied System Innovation*, 4(1):14, 2021.

[46] Annick AA Timmermans, Henk AM Seelen, Richard PJ Geers, Privender K Saini, Stefan Winter, Juergen Te Vrugt, and Herman Kingma. Sensor-based arm skill training in chronic stroke patients: results on treatment outcome, patient motivation, and system usability. *IEEE Transactions on Neural Systems and Rehabilitation Engineering*, 18(3):284–292, 2010.

[47] Christina Mittag, Vivian Waldheim, Axel Krause, and Thomas Seel. Using a single inertial sensor to control exergames for children with cerebral palsy. In *Current Directions in Biomedical Engineering*, volume 8, pages 431–434. De Gruyter, 2022.

[48] Smartsuit pro ii.

[49] Teslasuit documentation.

[50] Elisa Galofaro, Erika D'Antonio, Nicola Lotti, and Lorenzo Masia. Rendering immersive haptic force feedback via neuromuscular electrical stimulation. *Sensors*, 22(14):5069, 2022.

[51] Polona Caserman, Clemens Krug, and Stefan Göbel. Recognizing full-body exercise execution errors using the teslasuit. *Sensors*, 21(24):8389, 2021.

[52] Teslasuit user guide.

[53] George Rab, Kyria Petuskey, and Anita Bagley. A method for determination of upper extremity kinematics. *Gait Posture*, 15(2):113–119, 2002.

[54] Valeria Longatelli, Diego Torricelli, Jesús Tornero, Alessandra Pedrocchi, Franco Molteni, José L Pons, and Marta Gandolla. A unified scheme for the benchmarking of upper limb functions in neurological disorders. *Journal of neuroengineering and rehabilitation*, 19(1):1–20, 2022.

[55] Luiz A Knaut, Sandeep K Subramanian, Bradford J McFadyen, Daniel Bourbonnais, and Mindy F Levin. Kinematics of pointing movements made in a virtual versus a physical 3-dimensional environment in healthy and stroke subjects. *Archives of physical medicine and rehabilitation*, 90(5):793–802, 2009.

[56] Bonnie R Swaine, Johanne Desrosiers, Daniel Bourbonnais, and Jean-Louis Larochelle. Norms for 15-to 34-year-olds for different versions of the finger-to-nose test. *Archives of physical medicine and rehabilitation*, 86(8):1665–1669, 2005.

[57] Ge Wu, Frans C.T. van der Helm, H.E.J. (DirkJan) Veeger, Mohsen Makhsous, Peter Van Roy, Carolyn Anglin, Jochem Nagels, Andrew R. Karduna, Kevin McQuade, Xuguang Wang, Frederick W. Werner, and Bryan Buchholz. Isb recommendation on definitions of joint coordinate systems of various joints for the reporting of human joint motion—part ii: shoulder, elbow, wrist and hand. *Journal of Biomechanics*, 38(5):981–992, 2005.

## Abstract in lingua italiana

L'ictus rappresenta una delle principali cause di mortalità e disabilità nell'Unione Europea, spesso causando emiparesi degli arti controlaterali rispetto alla lesione cerebrale. La riabilitazione post-ictus è di fondamentale importanza per il ripristino delle funzioni neuromuscolari e il raggiungimento dell'indipendenza nelle attività quotidiane. Negli ultimi anni, dispositivi integrati all'avanguardia hanno cominciato a emergere come promettenti strumenti in questo ambito. Un esempio significativo è la Teslasuit, una tuta che unisce sistemi di Stimolazione Elettrica Neuromuscolare, di Motion Capture basato su sensori IMU e la Realtà Virtuale.
La presente ricerca si propone di esplorare il potenziale della Teslasuit nella riabilitazione degli arti superiori di pazienti post-ictus, con l'obiettivo di convalidarne l'efficacia e valutarne l'applicabilità in ambito medico. Questo studio presenta protocolli di convalida sia per il sistema di Motion Capture della Teslasuit che per il sistema di stimolazione elettrica, oltre a proporre un protocollo di esercizi imitation-based, ispirati alla Mirror Therapy, da svolgere interagendo con ambienti di Realtà Virtuale.
I nostri risultati, ottenuti dalla valutazione di 5 soggetti sani per ciascun protocollo, confermano la precisione e l'accuratezza nel monitoraggio dei movimenti del sistema di Motion Capture integrato nella Teslasuit, così come l'efficacia del suo sistema di stimolazione elettrica, presentato come un potenziale strumento per la riabilitazione neuromotoria. I dati dimostrano inoltre che sia possibile l'integrazione di questi sistemi con la VR. Da questa ricerca emerge chiaramente che la Teslasuit si configura come un dispositivo promettente per l'implementazione di terapie versatili e innovative nel contesto della riabilitazione neuromotoria dell'arto superiore.



**Parole chiave:** SEF; Teslasuit; motion capture; realtà virtuale; sistemi integrati indossabili



## Acknowledgements

We would like to express our gratitude to our thesis advisor, Professor Ambrosini, for the opportunity of taking part to this interesting project, her guidance, and expertise throughout the course of our research.
We would also like to extend our appreciation to our tutor, Francesca Dell'Eva, whose assistance has been instrumental in our thesis journey.
We are grateful for their contributions to our academic and personal development.